



Developing novel anti-*Candida* therapies through the understanding of drug-resistance mechanisms and by tailoring new chemicals to be used in anti-biofilm surfaces

Maria Joana Faustino Pinheiro

Thesis to obtain the Master of Science Degree in

Biotechnology

Supervisor(s): Prof. Dr. Nuno Gonçalo Pereira Mira

Prof. Dr. Maria Fernanda Do Nascimento Neves de Carvalho

Examination Committee

Chairperson: Prof. Dr. Miguel Nobre Parreira Cacho Teixeira

Supervisor: Prof. Dr. Nuno Gonçalo Pereira Mira

Member of the Committee: Prof. Dr. Jorge Humberto Gomes Leitão

November 2019

Preface

The work presented in this thesis was performed at the Institute for Bioengineering and Biosciences of Instituto Superior Técnico (Lisbon, Portugal), during the period January-September 2019, under the supervision of Prof. Dr. Maria Fernanda Do Nascimento Neves de Carvalho and Prof. Dr. Nuno Gonçalo Pereira Mira.

Declaration

I declare that this document is an original work of my own authorship and that it fulfills all the requirements of the Code of Conduct and Good Practices of the Universidade de Lisboa

Agradecimentos

Em primeiro lugar, gostaria de agradecer ao Professor Nuno Mira por ter aceite este desafio, por me ter disponibilizado esta oportunidade e por me ter guiado e desafiado ao longo deste projeto de forma exemplar. Agradeço igualmente à Professora Fernanda pelo tempo investido em mim a orientar e ensinar, de forma também exemplar, numa área que pouco dominava, a da síntese e caracterização química. Tenho de agradecer também à Marta Alves que se juntou a nós a meio do projeto para tentar uma abordagem inovadora e sem garantias. Guiou-me também exemplarmente e permitiu-me explorar a área dos materiais totalmente nova para mim, sempre confiante que iríamos alcançar bons resultados. Obrigada aos três pelas condições de trabalho que me foi permitido ter, pela confiança e incentivo.

Agradeço também à Joana pela síntese dos compostos, pela disponibilidade sempre que precisei, por tudo o que me ensaiou e por todas as conversas. Tenho de agradecer também à Maria João, Nuno Pedro e Sara por toda a paciência que tiveram sempre que tive dúvidas e dificuldades no trabalho laboratorial. Aos meus colegas de laboratório e amigos Inês, Fernão, João e Catarina agradeço também a ajuda quando precisei, os favores, as conversas, os desabafos e os momentos de descontração. Às minhas amigas Andreia, Rita, Mariana e Cristiana, cuja amizade foi crescendo à medida que as dificuldades iam surgindo ao longo do mestrado e sem as quais todo este percurso tinha sido muito mais difícil.

Finalmente, quero também agradecer aos meus pais e irmã por todo o apoio, confiança e perseverança que me transmitiram ao longo destes anos de faculdade. Por fim, um especial obrigado ao Miguel pela paciência e incentivo nos momentos de frustração, pela segurança sempre que senti que ia falhar e pelo encorajamento constante.

Abstract

The fungi belonging to the *Candida* genus are commensals of the human microbiome, however, when the host immune system is compromised these yeasts can overgrow causing infections that can be life-threatening. Besides, being well adapted as human-infecting microbes, *Candida* cells are able to acquire resistance to usual antifungals. Therefore, it is urgent the discovery of new molecules with antifungal activity. In this work, several camphorimine-based complexes having silver, copper and zinc as metallic centers, were synthesized, characterized and their activity against *Candida* strains, including those resistant to azoles, tested. Two promising Ag(I)-camphorimine complexes (P and Q) were identified. The MIC value calculated for compound P was 15.63 µg/mL either for *C. albicans* and *C. glabrata* while for compound Q was 31.25 µg/mL. Exploring functionalized polycaprolactone coatings with both compounds, it was possible to reduce colonization of stainless steel plates by 62% and 25%, comparing with colonization obtained in non-functionalized plates. These observations strongly suggest these compounds have a strong potential to be used as anti-*Candida* molecules including in biofilm-free surfaces, this being an important trait since colonization of medical devices is a critical factor underlying the success of *Candida* as pathogen.

Furthermore, the azole-resistance phenotype of two *C. albicans* isolates was scrutinized and results suggested that these isolates have a reduced fitness that renders them more able to cope with azole-induced stress. The ability of *C. albicans* to tolerate antifungals is increasingly reported and it is urgent to detect these fraction of growth subpopulations to ensure the most effective treatment.

Key-words: *Candida* • Ag(I)-camphorimine complexes • Functionalized coatings • Resistance • Fraction of growth

Resumo

Os fungos pertencentes ao género *Candida* são comensais do microbioma humano, contudo, quando o sistema imunitário do hospedeiro é comprometido, podem crescer em demasia, causando infecções que podem ser fatais. Além disto, sendo patogéneos humanos, as células de *Candida* são capazes de adquirir resistência aos antifúngicos usuais. Assim, é urgente a descoberta de novas moléculas com atividade antifúngica. Neste trabalho, foram sintetizados vários complexos à base de canforimina, tendo prata, cobre e zinco como centros metálicos, caracterizados e testada a sua atividade contra estirpes de *Candida*, incluindo resistentes a azóis. Dois complexos promissores de Ag(I)-canforimina (P e Q) foram identificados. O valor de MIC calculado para o composto P foi de 15,63 µg/mL para *C. albicans* e para *C. glabrata*, e para o composto Q foi de 31,25 µg/mL. Explorando revestimentos de policaprolactona funcionalizados com os compostos, foi possível reduzir a colonização de chapas de aço inoxidável em 62% e 25%, comparando com a colonização obtida em chapas não funcionalizadas. Estas observações sugerem que estes compostos têm potencial como moléculas anti-*Candida*, inclusive aplicados em superfícies sem biofilme, uma característica importante na colonização de dispositivos médicos subjacente ao sucesso enquanto patogéneo.

Além disto, o fenótipo de resistência aos azóis de dois isolados de *C. albicans* foi estudado e os resultados sugeriram que têm um fitness reduzido tornando-os hábeis em lidar com o stress induzido. A capacidade em tolerar antifúngicos é cada vez mais descrita em *Candida* e é urgente detectar estas frações de crescimento na população para garantir o melhor tratamento.

Palavras-chave: *Candida* • Complexos de Ag(I)-canforimina • Revestimentos funcionalizados • Resistência • Frações de crescimento

Table of contents

Preface	iii
Declaration	v
Agradecimientos	vii
Abstract	ix
Resumo	xi
Table of contents	xiii
List of figures	xv
List of tables	xix
Abbreviations.....	xxi
1 Introduction	1
1.1 Overview.....	1
1.2 An overview on antifungal resistance among <i>Candida</i> spp. and its consequences.....	3
1.3 Overview on the non-conventional approaches considered for the treatment of candidiasis..	5
1.4 Chemical synthesis: a growing option to obtain new antifungal molecules.....	9
1.4.1 Preventing candidiasis by avoiding colonization of medical devices by <i>Candida</i> spp.....	11
1.5 Introduction to the theme of the thesis.....	14
2 Materials and methods.....	15
2.1 Synthesis and chemical characterization of the camphorimine complexes	15
2.1.1 Materials	15
2.1.2 Synthesis of Ligands.....	15
2.1.3 Synthesis of Complexes	15
2.1.4 Chemical characterization	17
2.2 Strains and growth media used in the susceptibility assays	17
2.2.1 Assessment of antifungal potential of the camphorimine complexes.....	17
2.2.2 Assessment of synergistic effect of Ag(I) camphorimine complexes with fluconazole in <i>C. albicans</i>	18
2.2.3 Coating functionalization of stainless steel plates with Ag(I)-camphorimine complexes...	18
2.2.3.1 Physical-chemical characterization of the surfaces	18

2.2.3.2	Assessment of the effect of PCL coatings on the ability of <i>C. albicans</i> to form biofilms on the surface of stainless steel plates	19
2.2.4	Determination of MICs to fluconazole	19
2.2.5	Qualitative assessment of the FoG population in isolates 10A, 22CL and SC5314.....	20
3	Results and Discussion	21
3.1	“Re-design” of Ag(I)-based camphorimine complexes and assessment of their anti- <i>Candida</i> potential.....	21
3.2	Synthesis of ligands and of Zn- and Cu- based complexes and assessment of their anti- <i>Candida</i> potential	25
3.3	Ability of Ag(I)-based camphorimine complexes to act against azole-resistant <i>Candida</i> strains and its synergistic effect with fluconazole.....	29
3.4	Using Ag(I)-based camphorimine complexes in the design of new coatings for functionalizing medically relevant surfaces	32
3.5	Elucidating drug response behaviour <i>C. albicans</i> isolates 10A and 22CL.....	39
4	Final Remarks and Future Perspectives	44
5	References.....	46
6	Annexes	53
	Annex A.....	53
	Annex B.....	55
	Annex C.....	57
	Annex D.....	58
	Annex E.....	59
	Annex F.....	60
	Annex G	61
	Annex H.....	61

List of figures

Figure 1 – Distribution in percentage of <i>Candida</i> strains responsible for causing invasive infections. (In Perfect et al. 2017)	1
Figure 2 - Diversity of possible targets of antifungal compounds in cell fungi. These molecules can attack fungus-specific components of the cell wall or cell membrane, or metabolic processes. Conventional antifungal classes are indicated in dark blue boxes, redesigned drugs in purple and investigational antifungal agents are in light blue boxes. (Adapted from Perfect et al. 2017)	2
Figure 3 – Disk diffusion assay where RAD is the radius of the growth inhibit zone. The growth inside the zone of inhibition correspond to FoG. These measurements should be made using the software diskImageR, which evaluates the intensity of the image pixels. (Retrieved from Rosenberg et. al., 2018.) ^[11]	4
Figure 4 - Hypotheses of possible mechanisms of silver action in the cell that cause its death. Events that are believed to occur are highlighted: accumulation of nanoparticles in the cell wall and consequent formation of pores, reaction of silver with thiol groups of proteins and enzymes, and with the groups of phosphorus of the DNA chain. The formation of reactive oxygen species and free radicals is a consequence of all these events in the cell. (Adapted from Shao et al. 2007). ^[49]	8
Figure 5 - Image of star shaped Nanosilver under transmission electron microscope. In Sholkamy et al. (2019) ^[45]	9
Figure 6 - Possible mechanism of transmission of pathogens directly into the bloodstream through contaminated medical instruments. (Adapted from Pappas et. al. 2018). ^[58]	11
Figure 7 - Cross section of catheter shows active release of silver ions from all catheter surfaces and into the surrounding environment, providing antimicrobial protection. (Retrieved from Oligon™) ^[60] ...	12
Figure 8 - Mechanism of formation of polymer matrix nanocomposite. In Nivethaa et al. (2015). ^[65] ...	13
Figure 9 - Camphorimine (L1-L6) and camphor-sulfonylamine (L7,L8) derivatives used as ligands. Ligands marked with * were synthesized by Joana Costa.	21
Figure 10 - Reactional schemes for the synthesized ligands: L1, L2 and L3.	22
Figure 11 - FTIR spectrum of complex P, showing bands respective to O-H, C=O and C=N bonds. ...	22
Figure 12 - ¹ H NMR spectrum of complex P (detailed characterization in experimental section), showing the characteristic chemical shifts of the hydrogen atoms respective to the C ₆ H ₄ , H and CH ₃ groups..	23
Figure 13 - ¹³ C NMR spectrum of complex P (detailed characterization in experimental section), showing the characteristic chemical shifts of the several carbon atoms.	23
Figure 14 - Microdilution assay for complex P against the reference species (A) <i>C. albicans</i> SC5314 and (B) <i>C. glabrata</i> CBS138. The MIC value is indicated by an orange arrow and the 50% reduction of the growth registered in the absence of the chemicals is indicated by the orange line.	24
Figure 15 - Reactional schemes for the synthesized complexes of Cu(II), Cu(I) and Zn(II).	26
Figure 16 - MIC values (µg/mL) of the complexes P and Q, obtained for the reference <i>C. albicans</i> (SC5314) strain and respective isolates, represented by ●, and for the reference <i>C. glabrata</i> (CBS138) strain and respective isolates, represented by ■. The reference strains are represented by empty symbols. The most tolerant strains have the highlighted name.	29

Figure 17 - Microdilution assay for all the complexes P and Q against the azole resistant isolates of *C. albicans* 10A and 22CL. The MIC value is indicated by an orange arrow and the 50% reduction of the growth registered in the absence of the chemicals is indicated by the orange line30

Figure 18 - Heatmaps obtained in the synergism assay used to assess the potential of the synergistic effect of fluconazole and camphorimine compounds P and Q against the reference strain for *C. albicans* (SC5314) and resistant isolates of the same strain, 10A and 22CL. Dark green corresponds to a higher and dark red to reduced growth. FICI correspond to the fractional inhibitory concentration index and the values calculated indicate no interaction.31

Figure 19 - Scanning electron microscopy (SEM) micrographs for (A, C) and corresponding X-ray energy dispersive spectrometer (EDS) maps (B, D) for compound P (A, B) and compound Q (C,D) in powder; In EDS maps silver (Ag) is marked in red and carbon (C) in green.32

Figure 20 - Solubility of compounds P and Q in trifluoroacetic acid (TFA), chloroform and dichloromethane. Complete dissolution (+) and incomplete dissolution with precipitate formation (-). .33

Figure 21 - Photographs of PCL 8% broken coatings using TFA (A) and chloroform (D) as solvents. Scanning electron microscopy (SEM) micrographs of PCL 8% coatings using TFA (B,C) and chloroform (E, F) as solvents.33

Figure 22 - Photographs of PCL 4% coatings using chloroform (A) and dichloromethane (D) as solvents. Scanning electron microscopy (SEM) micrographs of PCL 4% coatings using chloroform (B,C) and dichloromethane (E, F) as solvents.34

Figure 23 - Graphical representation of CFUs/mL values obtained for each plate in the supernatant and biofilm in the assays using chloroform and dichloromethane as solvent. The results shown are means of, at least, three independent experiments. Bars represent average errors. Plates tested were: bare plate, PCL coated plate, PCL plate and compound P at concentrations of x10 MIC values ($\mu\text{g/mL}$) (P10) and PCL plate and compound Q at concentrations of x10 MIC values ($\mu\text{g/mL}$) (Q10).35

Figure 24 - Photographs of PCL 4% coatings using chloroform as solvent, without compounds (A) and with compound P (D) or Q (G) at concentrations of x10 MIC values ($\mu\text{g/mL}$). Scanning electron microscopy (SEM) micrographs of PCL 4% coatings using chloroform as solvent, without compounds (B,C) and with compound P (E,F) or Q (H,I) at concentrations of x10 MIC values ($\mu\text{g/mL}$). Points X and Y mark structures on the coating in which silver was detected.....36

Figure 25 - Colonization of bare and coated steel surfaces by *C. albicans* SC5314 incubated under simulated physiological conditions and corresponding micrographs from SEM: Bare plate (A); PCL coated plate (B); PCL plate and compound P (C) or compound Q (D) at x10 MIC values ($\mu\text{g/mL}$).37

Figure 26 - Colonization of bare and coated steel surfaces by *Candida albicans* SC5314 incubated under simulated physiological conditions and corresponding micrographs from SEM: PCL coated plate and compound P (A) or compound Q (B, D) at x100 MIC values ($\mu\text{g/mL}$). (C): graphical representation of colony forming units per milliliter (CFUs/mL) values obtained for supernatant and biofilm using chloroform as solvent. The number of CFUs in biofilm was quantified after washing and scratching the surface. The number of CFUs present in the supernatant of the cultures that were in contact with the

biomaterial was also determined. (D) SEM micrographs of large structures formed by cells and silver particles dispersed on the surface of Q100 coating38

Figure 27 - Microdilution assay for fluconazole against *C. albicans* reference strain SC5314 and strains 10A and 22CL. The MIC value is indicated by an orange arrow and the 50% reduction of the growth registered in the absence of the drug is indicated by the orange line.....39

Figure 28 - Microdilution assay for fluconazole in concentrations of 0, 16, 64 and 128 µg/mL, against *C. albicans* reference strain SC5314 and strains 10A and 22CL. The 50% reduction of the growth registered in the absence of drug is indicated by the orange line for strain SC5314, black line for strain 10A and broken line for strain 22CL.40

Figure 29 – Observation of cells of strains SC5314, 10A and 22CL under the light microscope after the microdilution assay. Cells exposed to 0 (control), 16 and 128 µg/ml fluconazole were observed (A). Graphical representation of CFUs/mL values obtained for strains SC5314, 10A and 22CL after the microdilution assay with fluconazole concentrations of 0, 16, 64 and 128 µg/mL. The results shown are means of, at least, three independent experiments. Bars represent average errors. (B)41

Figure 30 - MHA disk diffusion assay images for strains SC5314, 10A and 22CL in control and in contact with fluconazole. Images on fluconazole discs zoom into the zone of inhibition.....42

Figure 31 - Microdilution assay for all the complexes (A-T) against the reference species *C. albicans* SC5314. The MIC value is indicated by an orange arrow and the 50% reduction of the growth registered in the absence of the chemicals is indicated by the orange line.56

Figure 32 -Microdilution assay for all the complexes (A-T) against the reference species *C. glabrata* CBS138. The MIC value is indicated by an orange arrow and the 50% reduction of the growth registered in the absence of the chemicals is indicated by the orange line58

Figure 33 - Microdilution assay for all the complexes P against the azole resistant isolates of *C. glabrata* (3-12). The MIC value is indicated by an orange arrow and the 50% reduction of the growth registered in the absence of the chemicals is indicated by the orange line.58

Figure 34 - Microdilution assay for all the complexes Q against the azole resistant isolates of *C. glabrata* (3-12). The MIC value is indicated by an orange arrow and the 50% reduction of the growth registered in the absence of the chemicals is indicated by the orange line59

Figure 35 - Graphic representation of the ODs obtained in the assays to assess the effects of the potential synergistic combination of compound P or Q and fluconazole against *C. albicans* SC5314, 10A and 22CL strains. In the graphic are represented a control column (w/o FLC or A) with the growth medium without stress, the medium supplemented only with compounds P or Q, only with FLC and the conditions under which stresses were combined. Two non-inhibitory concentrations of compounds P and Q were used, 0.98 µg/mL, 1.95 µg/mL and two non-inhibitory concentrations of FLC were used, 0.063 µg/mL and 0.125 µg/mL.60

Figure 36 - Growth curve of SC5314, 10A and 22CL strains in RPMI growth medium (at pH 7). Growth of the different strains was based on the increase of OD600nm of the culture. The growth curves shown are representative of at least three independent experiments that resulted in a similar growth pattern.61

List of tables

Table i – New approaches in the search for new antifungal agents that fill the reduced number of effective drugs, along with their descriptions and some examples.	5
Table ii - Examples of complexes with high to moderate anti-candida activity; where DIZ, represents diameter of inhibition zone. Adapted from Salazar et al. (2018) ^[13]	10
Table iii - MIC values ($\mu\text{g}/\text{mL}$) of the ligands, precursors and silver complexes against <i>C. albicans</i> (SC5314) and <i>C. glabrata</i> (CBS138), based on the EUCAST microdilution method. The complexes P, Q, R, S and T were synthesized by someone else.....	24
Table iv - MIC values ($\mu\text{g}/\text{mL}$) of the precursors and copper and zinc complexes against <i>C. albicans</i> (SC5314) and <i>C. glabrata</i> (CBS138), based on the EUCAST microdilution method. The complexes B, D, E, K, M, N and O were not synthesized during the course of this work and were already available in the CQE laboratory.....	27
Table v - Ratios between the CFUs/ mL values obtained in each assay and the values for the bare plates, in both supernatant and biofilm. PCL solvents were chloroform and dichloromethane and the various variants tested were: bare plate, PCL coated plate, PCL plate and compound P at concentrations of x10 and x100 MIC values ($\mu\text{g} / \text{mL}$) (P10 and P100 respectively) and PCL plate and compound Q at concentrations of x10 and x100 MIC values($\mu\text{g} / \text{mL}$) (Q10 and Q100 respectively).....	35
Table vi - Summary of the strategy followed in the functionalization of PCL coating.	61

Abbreviations

ABC	ATP-Binding Cassette
AMPs	Antimicrobial peptides
<i>C. albicans</i>	<i>Candida albicans</i>
<i>C. glabrata</i>	<i>Candida glabrata</i>
<i>C. krusei</i>	<i>Candida krusei</i>
<i>C. parapsilosis</i>	<i>Candida parapsilosis</i>
<i>C. tropicalis</i>	<i>Candida tropicalis</i>
CFU	Colony Forming Units
cDNA	Complementary Deoxyribonucleic Acid
ddH₂O	Double Distilled Water
DMSO	Dimethyl Sulfoxide
DNA	Deoxyribonucleic Acid
dNTP	Deoxyribonucleotide Triphosphates
EA	Elemental analysis
EDS	Energy Dispersion Spectrometer
EUCAST	European Committee on Antimicrobial Susceptibility Testing
FICI	Fractional Inhibitory Concentration Index
FLC	Fluconazole
FoG	Fraction of Growth
FTIR	Fourier Transform Infrared Spectroscopy
IC₅₀	Half maximal inhibitory Concentration
MHB	Mueller Hinton Broth
MM	Minimal Medium

MIC	Minimum Inhibitory Concentration
NCAC species	Non- <i>Candida albicans</i> <i>Candida</i> species
NMR	Nuclear Magnetic Resonance
OD	Optical Density
PBS	Phosphate Buffered Saline
PCL	Polycaprolactone
RNA	Ribonucleic Acid
RNAi	Interference Ribonucleic Acid
ROS	Reactive Oxygen Species
RPM	Rotations per Minute
RPMI	Roswell Park Memorial Institute
RT	Room Temperature
SEM	Scanning Electron Microscopy
spp.	Species
SS	Stainless Steel
YPD	Yeast Peptone Dextrose

1 Introduction

1.1 Overview

Candida are eukaryotic, unicellular microorganisms, members of the Fungi kingdom. Some species of the *Candida* genus are exclusive to the human microbiome and can be found in the normal microbiota of an individual's mucosal oral cavity, gastrointestinal and genitourinary tracts and skin, such as *C. albicans* and *C. parapsilosis*, while others species are also scattered in the environment, like *C. glabrata*.^[1] Those species found in the human microbiota are considered commensal in healthy humans, which means that they live and thrive thanks to the resources of the host, while the host does not benefit nor is harmed in this association. However, when mucosal barriers are disrupted, the immune system is compromised or when changes occur in the host microbiota, the commensal *Candida* populations transit to a pathogenic phase, invading the bloodstream and causing potentially lethal infections with the overall mortality ranging from 30% to 60%.^[2] Factors such as treatment with antibiotics, diabetes, cancer, extreme age, immunosuppression, intravenous catheters or long-term hospitalization pose a higher risk of getting a fungal infection caused by *Candida*. Reports have also been made concerning the possibility of exogenous transmission of *Candida* to patients via contamination of hospital materials or through contact with healthcare providers.^[3]

Around 17 different *Candida* species are known to cause infections, however the majority of the invasive infections (that is, those in which the yeasts colonise the bloodstream) are attributable to *C. albicans*, followed by *C. tropicalis*, *C. parapsilosis*, *C. glabrata* and *C. krusei*.^[4] Among these, *Candida albicans* is the leading causative species of disease, but the other species (generally known as non-*Candida albicans*, *Candida* or NCAC) are emerging, in some cases surpassing *C. albicans*. Among NCAC, *Candida glabrata* is of particular concern due to its high ability of rapidly acquiring resistance to the antifungals used in treatments.^[5]

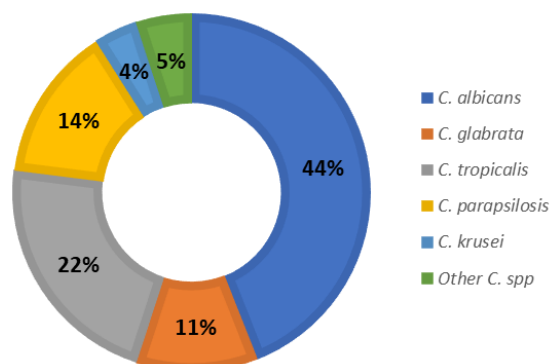


Figure 1– Distribution in percentage of *Candida* strains responsible for causing invasive infections. (In Perfect et al. 2017)

At this moment, there are four drug classes available for the treatment of *Candida* infections: azoles, polyenes, echinocandins and the pyrimidine analogue flucytosine (Figure 2). These drugs explore the differences between the pathogen and the host organism, acting in particular in metabolism of ergosterol (azoles and polyenes) and in biosynthesis of the cell wall (echinocandins). This limited panoply of options is alarming since the chances of a successful treatment decrease and increases the possibilities of a fatal outcome if the pathogen is resistant to one or multiple drugs. Since both mammalian cells and yeast cells are eukaryotic, often antifungal drugs end-up having hard side effects, including toxicity to the liver or to the kidney.^[5]

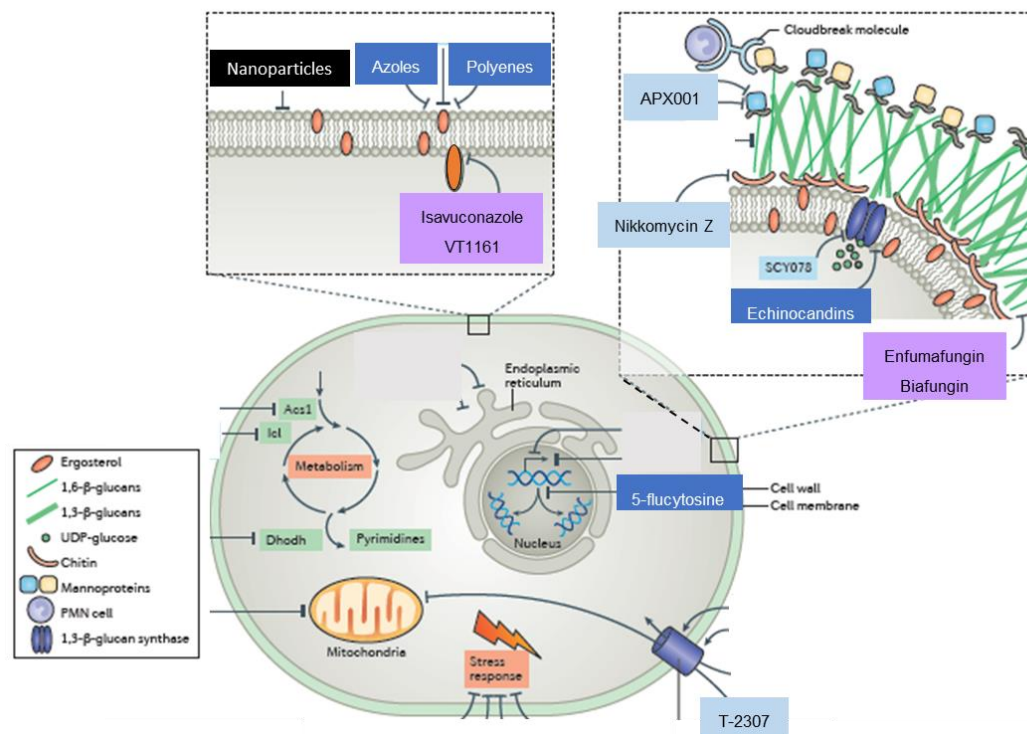


Figure 2 - Diversity of possible targets of antifungal compounds in cell fungi. These molecules can attack fungus-specific components of the cell wall or cell membrane, or metabolic processes. Conventional antifungal classes are indicated in dark blue boxes, redesigned drugs in purple and investigational antifungal agents are in light blue boxes. (Adapted from Perfect et al. 2017)

The efficacy and the incidence of resistance concerning the different antifungals is variable among the different *Candida* species. Susceptibility testing demonstrated a significant decrease on the rates of susceptibility to azoles among *Candida* species, from 65.2% in 2011 to 60.6% in 2015. Among the infection-causative species mentioned above, resistance rates increased by 0.4% for *C. albicans* and 9.1% for *C. glabrata* during these four years.^[6] Some of the genetic and molecular mechanisms underlying resistance to antifungals have been documented in some of the identified resistant *C. albicans* or *C. glabrata* strains, this knowledge being essential to guide the design of more effective therapies; nonetheless, till this day resistant strains whose underlying mechanism is not known continue to be identified.^[7] Despite the clinical relevance of drug resistance in the context of yeast infections, this subject remains poorly studied, in comparison with antibiotic resistance in bacterial pathogens. Some of the insights gathered until so far are detailed in the next section.

1.2 An overview on antifungal resistance among *Candida* spp. and its consequences

In general, fungi infect billions of people every year and the resulting effects on human health are spiralling, however, fungi remain largely under-appreciated as human pathogens. Currently the overall mortality rate for fungal diseases surpasses that for breast cancer or malaria and can be compared to that of HIV or tuberculosis.^[7] Today we are seeing a rise in the number of cases of fungal infections and the use of antifungals follows this trend. However, the frontline treatments for fungal diseases we use today may be ephemeral, since fungi reproduce rapidly, have highly dynamic and plastic genomes and the range of drugs available is very limited.^[8] This combination justifies the increasing number of resistant species reports. The first step is the identification of the resistant strains. For that, the European Committee on Antimicrobial Susceptibility Testing (EUCAST) has used the definitions of susceptible or resistant to a given antifungal to categorize the microorganisms as treatable or not treatable with that drug. A microorganism is categorized as “susceptible when there is a high likelihood of therapeutic success using a standard dosing regimen” of the agent, or as “resistant when there is a high likelihood of therapeutic failure even when there is increased exposure to the agent”, and this classification is measured as minimal inhibitory concentration (MIC) after 24 hours of growth in the presence of the selected drug.^[9] Fungal infections generally follow the “90/60” rule for predicting therapeutic outcomes based in *in vitro* susceptibility testing: ~90% of susceptible isolates and ~60% of resistant isolates respond to therapy, which implies that infection outcomes are influenced by features of the pathogen as well as host factors that are not reflected by the MIC.^[10] This link between the identification of resistant strains and an outcome brings to light the important issue that is to phenotype the strains in a rapid, fast and accurate manner as this might play a critical role in the patient outcome. As said above, phenotype of the strain relies on the identification of the MIC (corresponding to the lowest concentration of drug that results in 50% growth inhibition, compared to the growth that is observed in drug-free conditions). These MIC measurements have been optimized to minimize or ignore tolerance phenomena, *i.e.* to ignore residual fungal growth focusing only growth above inhibitory concentrations.

In fact, this tolerance singularity has already been described: within a cell population there is a subpopulation that can grow slowly in the presence of stress. In the work of Rosenberg *et. al.* (2018)^[11], they found a outlandish behavior in *C. albicans* isolates and called it tolerance, that can be quantified as the growth fraction (FoG) above the MIC and is different from susceptibility/resistance. This ability appears to result from drug response strategies that allow cells to grow slowly despite the drug's ability to interact with its target and to remain in the cell, differing from resistance mechanisms that affect the drug target or its concentration in the cell. This subpopulation effect of tolerance is readily detected on disk diffusion assays and correspond to the colonies that growth within the zones of inhibition (Figure 3) and medical procedures state that these colonies should be ignored during therapy.^[3] However, Rosenberg *et. al.* (2018)^[11], concluded that these subpopulations are associated with persistent candidemia and also raise the issue that it is necessary to monitor parameters other than MIC, such as FoG, in clinical practice to detect these subpopulations and ensure the most effective therapy. Tolerance is detected in 25-60% of clinical isolates^[10] and highly tolerant isolates are associated with events of

persistent candidemia. ^[11] The importance of quantifying tolerance levels of clinical strains is therefore clear, and it is essential to identify other parameters to make the susceptible/resistant classification more assertive and accurately predict the response of the isolate to the proposed treatment.

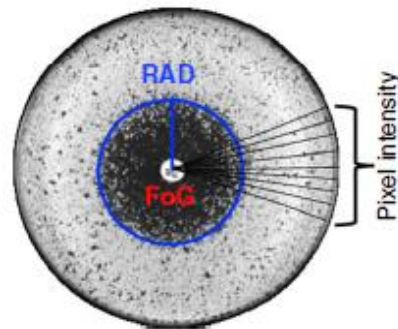


Figure 3 – Disk diffusion assay where RAD is the radius of the growth inhibit zone. The growth inside the zone of inhibition correspond to FoG. These measurements should be made using the software diskImageR, which evaluates the intensity of the image pixels. (Retrieved from Rosenberg et. al., 2018.)^[11]

Besides the population heterogeneity, the variation in the mechanisms by which *Candida* species can outweigh drug effects pose a significant challenge, not only in determining the efficacy of the therapy, but also in the early diagnosis of the infection. Reports on resistance to antifungal agents is much more common among the azoles (especially fluconazole), which have been widely used to treat *Candida* infections.^[12] When we talk about resistance to antimicrobial several very general mechanisms are described, with the occurrence of mutations that alter the drug target, mostly reducing its efficacy, being one of the most well described to explain resistance to azoles among *C. albicans*.^[13] In specific, it has been found that a number of *C. albicans* strains resistant to azoles encode mutated alleles of the ERG11 gene, the target of azoles, that show reduced affinity for the drug. For *C. albicans*, over-expression of ERG11 has also been described as a mechanism driving resistance.^[13] However, in the case of *C. glabrata*, this mechanism is highly unusual with only one study correlating resistance to azoles with mutations in the coding sequence of CgERG11, suggesting that this species has evolved responses to handle azole stress distinct from those verified in *C. albicans*.^[13] The up-regulation in mechanisms promoting the efflux of the antimicrobial is another of the general mechanisms of resistance found in resistant strains. In the specific case of *Candida* species, the more studied drug efflux pumps linked to azole resistance are those belonging to the ATP-binding cassette (ABC) superfamily which include in *C. albicans* CaMdr1, CaCdr1 and CaCdr2^[14]; in *C. glabrata*, CgCdr1, CgCdr2 and CgPdh1^[15,16]. For *C. glabrata*, it was found that the transcriptional activation of the genes encoding these efflux pumps was mediated by a single Zn(2)-Cys(6) transcription factor – CgPdr1p, which binds to specific sequences present in the promoter region, promoting their up-regulation. The over-expression of drug-efflux pump-encoding genes results, mostly, from the emergence of activating mutations in the coding sequence of the corresponding regulators.^[17,18] An important feature of these hyper-active alleles is that they become active even when the azole drugs are not present which means that these isolates constitutively over-express the drug-efflux pumps.^[19]

Resistance either emerges in response to an antifungal selection pressure in the individual patient, especially in long prophylactic treatment, or, more rarely, occurs due to horizontal transmission

in hospitals of resistant strains among patients. Because azoles are not only used for human and animal health, but also for crop protection, timber protection and antifouling coatings, it is thought that the cross-talk between these different environments can have impact in the increasing evolution of resistance.^[12] Moreover, in response to the increasing demand for food quantity and variety, intensive agriculture is increasingly being applied for higher productivity, and with it a broad scale of pesticide application. In addition to controlling the spread of agricultural fungal pathogens, antifungal agents of the azole class play an important role in the management of human fungal diseases. This ubiquitous use of azoles has resulted in a parallel evolution of cases of resistance in clinical and phytopathogens fungi. More troubling is that very similar resistance mechanisms in *Candida* spp. are seen across field and clinic situations.^[20] These findings highlight how narrow the spectrum of antifungal drugs is and show that finding new drugs with new modes of action and targets other than those now attacked is essential to prevent cross-resistance and ensure fungal control mechanisms in the future.^[21]

1.3 Overview on the non-conventional approaches considered for the treatment of candidiasis

Besides the problems with resistance mentioned above, the “traditional” antifungals also have drawbacks in what concerns their toxicity, spectrum of activity, safety and pharmacokinetic properties. All these have been paving the way for the development of new molecules/approaches for the treatment of candidiasis, this being difficulted by the trouble in identifying unique targets in the yeast cells that could be absent in host cells, which like *Candida* are also eukaryotic cells and therefore conserve a lot of the basic molecular mechanisms of functioning. That is actually the reason why most antifungal drugs have significant off-target effects that are reflected in host toxicity. An overview on several new approaches that are nowadays being considered as alternatives to the more traditional treatments for candidiasis are summarized in Table i, including their description and mode of action. Further details on some of these approaches will be provided below.

Table i – New approaches in the search for new antifungal agents that fill the reduced number of effective drugs, along with their descriptions and some examples.

Approach	Description	Examples
Redesign of the usual drugs	Modifications to usual drugs to increase antifungal activity, reduce toxicity and drug interactions.	<ul style="list-style-type: none"> - Biafungin or CD101 has a chemical modification on the echinocandin backbone that makes the compound more stable with a similar activity to caspofungin against <i>Candida</i> species;^[22] - VT1161 belong to a novel class of triazoles and is about 1000-fold more selective for <i>Candida</i> CYP51 (enzyme) than for the human enzyme and has high

		efficacy against fluconazole-resistant <i>Candida</i> isolates. [23]
Use of natural compounds	The uneven availability, chemical diversity, structural complexity, lack of substantial toxic effects, and broad spectrum of antimicrobial activity of natural products, provide unlimited possibilities for new effective drugs or adjuvants. (Figure 2 in green)	<ul style="list-style-type: none"> - ASP2397 from the fermentation broth of fungal <i>A. Persicinum</i> MF-347833 strain. Showed activity against <i>C. glabrata</i> and was not cytotoxic for mammalian cells; [24] - Gallic acid and catechin had MIC values ranged from 0.156 to 1.250mg/ml against <i>C. albicans</i>, <i>C. tropicalis</i>, <i>C. parapsilosis</i> and <i>C. glabrata</i>; [25]
Probiotics	The live microorganisms administered affect the human microflora by competing with others for nutrients and binding sites, inhibiting their growth by producing microbicides and stimulating the immune response of the host organism. [27] (Figure 2 in orange)	<ul style="list-style-type: none"> - <i>Lactobacillus salivarius</i> secretes intermediates capable of inhibiting the formation of cariogenic <i>C. albicans</i> biofilm in oral cavity; [26] - <i>Saccharomyces cerevisiae</i> shows ability in fighting <i>Candida</i>; [27] - <i>Bacillus subtilis</i> might control <i>Candida</i> species in the oral cavity and the intestinal tract; [28]
Vaccination	The greatest advances in fungal vaccines are regarding studies of invasive candidiasis. Until now, vaccines under study demonstrated to be stable, immunogenic, harmless and have been shown to induce systemic and mucosal protective immunity. [29] (Figure 2 in grey)	<ul style="list-style-type: none"> - NDV-3A vaccine is in phase II and prevents fungal adhesion and invasion; [29] - Sap2 vaccine is under study to enter phase I; [30]
RNAi interference RNA	Methodology to knock down essential vital factor or virulence factor genes in the pathogens. (Figure 2 in yellow)	<ul style="list-style-type: none"> - Designing of a 19-nucleotide siRNA based on the cDNA sequence of the EFG1 gene in <i>C. albicans</i>. Hyphae formation was significantly reduced. [31]
Small-molecule	Possibility of small-molecule target specific sites in <i>Candida</i> cells and thereby compromise its viability. (Figure 2 in yellow)	<ul style="list-style-type: none"> - iKIX1 inhibited Pdr1-dependent gene activation and azole efflux pump expression was repressed. There was a re-sensitization of <i>C. glabrata</i> resistant to antifungal azole. [32]
AMPs antimicrobial peptides	Gene encoded, ribosome-synthesized peptides, less than 10 kDa, with an overall positive	<ul style="list-style-type: none"> - K40H derived from the constant region of human immunoglobulin M was able to act <i>in vitro</i> against <i>C. albicans</i>, including strains resistant to conventional

	charge and amphiphilic structure. Antimicrobial peptides show activity against viruses, fungi and bacteria. Due to their features, it moves rapidly to the site of infection and promotes the increase of microbial cytoplasmic membrane permeability. [33] (Figure 2 in white)	antifungal drugs and did not show toxic activity on mammalian cells; [34] - AMPs with natural origins like <i>Acanthoscurria gomesiana</i> spider [35], <i>Agelaia pallipes</i> wasp [36] and bovine lactoferrin [37] apparently cause changes in fungal membrane and β -1,3 glucan binding, or from plants such as <i>Trapa natans</i> [37] and <i>Arabidopsis thaliana</i> [38] interfere with the cell membrane and seems to cause downregulation of <i>ERG1</i> gene expression.
Nanoparticles	A microscopic particle with less than 100 nm. They display decreased size, enhanced specific surface area, and thus strengthened reactivity. [39]	Silver nanoparticles (AgNPs), zinc oxide nanoparticles (ZnONPs) and nanocarbons such as single-walled carbon nanotubes, multiwalled carbon nanotubes, and graphene materials are being studied and applied as possible antifungal agents. [39]

Chemical genomics-based screenings, redesign of approved drugs and high throughput screenings of natural products are some of the approaches being followed for the discovery of new antifungal molecules. In addition to these, other innovative approaches are also being explored, such as the use of probiotics.^[40] Recently, vaccination has also emerged as a possible alternative and a growing number of antifungal vaccine candidates are being evaluated in pre-clinical studies. [37,38] The use of genetic tools also seems to offer several possibilities as antifungal treatments, although in this case the implementation in the clinical setting is likely to be more difficult. The introduction of RNA silencing machinery in fungi has led to the promising application of RNAi methodology to knock down essential vital factor or virulence factor genes, as well as the application of small-molecules that target transcription factor binding site in the microorganisms.^[41] Antimicrobial peptides (AMPs) have also been considered as an option of antifungal therapy. These molecules are gene encoded, have less than 10 kDa and show activity against various microbes including viruses, fungi and bacteria. Due to their features of small size, an overall positive charge and amphiphilic structure, they can rapidly move to the site of infection and promote the increase in the permeability of the microbial cytoplasmic membrane by interacting with negatively charged lipids. One characteristic of AMPs that makes them a potential therapeutic agent is their naturally high selectivity, which allows, through electrostatic interactions, a more efficient binding to the membrane but not to the mammalian cells' plasma membrane.^[42] Several online databases [43] compile and catalogue natural and synthesized AMPs, with information on each peptide, its origin and its target.

The use of nanoparticles as vehicles for treating candidiasis has also been largely explored (in line to what is also observed concerning the generalization of nanoapproaches in treatment of diseases in general [44]) at this point, mostly from an academic point of view. These nanoparticles can be synthesized via chemical routes (the more traditional approach) but also using environmental-friendly

strategies (such as the use of plant extracts in a phytotherapeutics perspective ^[45]) and they have as great advantages their decreased size and enhanced specific surface area. ^[39] Probably, the highest number of applications involving the use of nanoparticles for treating candidiasis explores silver nanoparticles ^[39], this resorting to the very well-known antimicrobial properties of this metal. ^[46] The use of silver nitrate in wound treatment can be traced back to the 18th century, during which it was used in the treatment of ulcers. ^[47] More recently, clinicians started using wound dressings that incorporate varying levels of silver, including silver salts, silver nanoparticles and other silver compounds, that have been shown to act as antimicrobial agents. ^[48] Upon release, silver ions are thought to interact with thiol groups, carboxylates, phosphates, hydroxyls, imidazoles, indoles and amines, and multiple deleterious events and specific lesions simultaneously interfere with microbial processes. ^[38] Although the precise molecular mechanisms by which Ag-based nanoparticles exert their inhibitory action over *Candida* cells remains to be disclosed, it is known that these nanoparticles are able to anchor to the cell wall and subsequently penetrate it, thereby causing structural changes in the permeability of the cell membrane and causing death (Figure 4).^[49] The accumulation of the nanoparticles on the cell surface and the formation of free radicals by the nanoparticles is another mechanism believed to underlie toxicity of silver-based nanoparticles against *Candida* cells.^[50] It has also been proposed that release of silver ions by the nanoparticles can occur and these ions avidly bind to negatively charged components in proteins and nucleic acids, thereby affecting structural changes in cell wall, membranes and nucleic acids that affect viability.

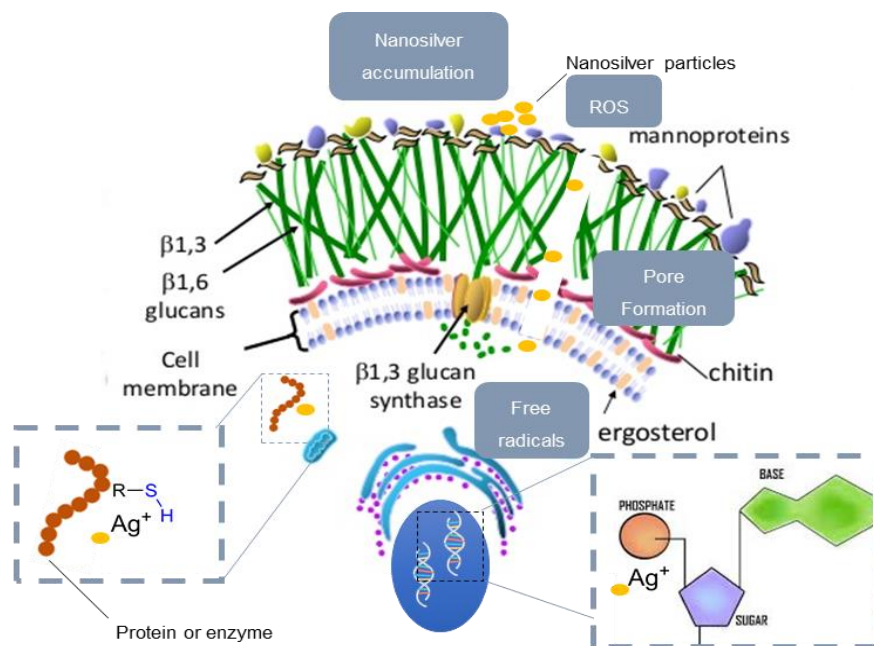


Figure 4 - Hypotheses of possible mechanisms of silver action in the cell that cause its death. Events that are believed to occur are highlighted: accumulation of nanoparticles in the cell wall and consequent formation of pores, reaction of silver with thiol groups of proteins and enzymes, and with the groups of phosphorus of the DNA chain. The formation of reactive oxygen species and free radicals is a consequence of all these events in the cell. (Adapted from Shao et al. 2007).^[49]

An interesting observation is the fact that silver-based nanoparticles can be produced using live cells as a reducing agent. This has been demonstrated for various microbes including filamentous fungi^[51] or even *C. albicans*^[52] or, more recently, a bacterial species that has been found biosynthesize star shaped silver nanoparticles as detailed in Fig.5^[45].

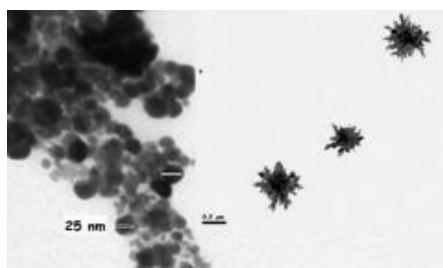


Figure 5 - Image of star shaped Nanosilver under transmission electron microscope. In Sholkamy et al. (2019)^[45]

1.4 Chemical synthesis: a growing option to obtain new antifungal molecules

In this area of research, where a large number of new molecules are being considered as antimicrobials, there is great interest in the use of metal complexes which are molecules composed by a metallic centre coordinated to an organic moiety. The properties of the complexes depend of the nature of the metal and ligands. In the coordination of an organic scaffold to a metal ion, the activity of the compound can be enhanced due to the stabilization provided by the metal center. In parallel, the toxicity of the metal may be reduced due to the shielding effect provided by the organic ligand that can limit the metal interaction with the surrounding biomolecules or targeted it towards the desired effects.^[53] As such, this combination gives rise to compounds with peculiar attributes, such as the ability to interact with DNA, enzymes and protein targets or redox features that can enable redox reactions, leading to the production of reactive species resulting in oxidative stress for the cells.^[54] Another possibility is the bio-reduction of the complex itself leading to the release of active metabolites. As can be expected, all these features together with the large diversity of bonding modes and structures can be explored in new formulations with antifungal properties providing a great versatility and creativity in the design of novel prospective drugs.^[55]

Based on this strategy, several molecules have been reported as having the ability to inhibit the growth of *Candida species*. Table ii summarizes some of the examples of these new compounds that have been identified as having a high-anti-*Candida* potential.^[13]

Table ii - Examples of complexes with high to moderate anti-candida activity; where DIZ, represents diameter of inhibition zone. Adapted from Salazar et al. (2018) ^[13]

Metal Center	Compound	Antifungal assessment (<i>C. albicans</i>)
Silver	Tetrazole nitrogen ligand	0.62 µg/mL MIC
	Phenanthroline ligand	1.2-11.3 ng/mL MIC
Cooper	Schiff base type ligand	4 µg/mL MIC
	Dendrimer ligand	1 mg/mL MIC
Cobalt	Ethylenediamine derivatives	62.5 µg/mL MIC
	Dendrimer ligand	0.6 mg/mL MIC
Nickel	Schiff base type ligand + 2,2'-bipyridine ancillary ligand	87 µg/mL MIC
	Dendrimer ligand	0.6 mg/mL MIC
Cadmium	Bidentate azodye ligand	17.1 mm DIZ
	Ferrocenyl chalcone derivatives	20 mm DIZ
Chromium	Bidentate azodye ligand	19.6 mm DIZ
	Ferrocenyl chalcone derivatives	15 mm DIZ (12 mm ligand inhibition)
Tin	Dithiocarbamate derivatives	2.5-250 µg/mL MIC
Manganese	Schiff base type ligand	51.8% inhibition (36% ligand inhibition)
Zinc	Schiff base type ligand + 2,2'-bipyridine ancillary ligand	102 µg/mL MIC
	Chromone hydrazine ligand	24.8 and 26.3 mm DIZ
Iron	Thiazole derivatives ligand	18.9 mm DIZ (11.9 mm ligand inhibition)
	Ferrocenyl chalcone derivatives	17 mm DIZ (12 mm ligand inhibition)
Ruthenium	Perylene ligand	12.5 ng/mL reduce to 50% the growth
Lead	Ferrocenyl chalcone derivatives	17 and 21 mm DIZ (12 and 19 mm ligand inhibition)
Barium	Ferrocenyl chalcone derivatives	13 mm DIZ (12 mm ligand inhibition)
Palladium	Phenylphosphine ligand	0.5 µg/mL MIC

As shown in Table ii, most of the metals that have been exploited are transition metals, of which silver is the most prominent and was previously described. Followed by silver comes palladium, tin, copper, cobalt, nickel and zinc. From these, zinc and copper are well-known for their biocompatibility, with important role in immunity and with demonstrated antimicrobial properties.^[56] Copper is an essential trace element in most living organisms and is present mostly in proteins and enzymes, where it serves as an electron donor/acceptor by alternating between the redox states Cu(I) and Cu(II), giving rise to ROS in chemical reactions in which it participates.^[57] Similar to copper, zinc is an essential element for proper functions of human body, can be readily excreted by natural biological processes. In addition, these two metals have the advantage of being easily accessible and cheaper than silver.^[39]

1.4.1 Preventing candidiasis by avoiding colonization of medical devices by *Candida* spp.

It has been well established that systemic infections caused by *Candida* species, specially by *C. albicans*, can result by the ability of these cells to colonize a number of medical devices ranging from prosthetics, pacemakers or catheters, which eventually serve as injection vehicles directly in the blood (Figure 6).^[58]

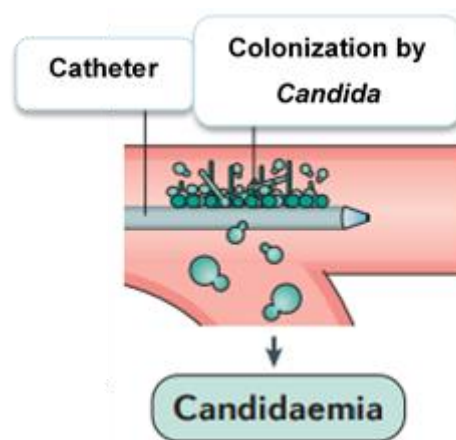


Figure 6 - Possible mechanism of transmission of pathogens directly into the bloodstream through contaminated medical instruments. (Adapted from Pappas et. al. 2018).^[58]

Under this scenario, several strategies have been designed to prevent colonization of medical devices by *Candida* species. One approach has been the impregnation or surface coating of the medical device surface with selected antimicrobial agents. This strategy was followed by Roe *et al.* (2008) that developed catheters coated with silver nanoparticles using AgNO₃, and the activity on microbial growth and biofilm formation was evaluated against pathogens most commonly involved in catheter-related infections, including *C. albicans* in which the inhibition of biofilm formation was almost complete.^[59] Another approach was used by the Edwards Lifesciences company that explored silver-carbon-platinum catheters (Figure 7 - Oligon™). In these devices iontophoretic polymers are designed to release silver ions when wet with body fluids by combining silver and platinum powders in the polymer composition.

Platinum, by having a greater electrochemical reduction potential attracts electrons from silver forming silver ions. One additional component was needed to allow the reactions to continue and silver ions to be released over the time, which was carbon that serves as an electrical conductor between metallic silver and platinum particles. *In vitro* testing demonstrated a broad spectrum of effectiveness against several pathogenic organisms, like *C. albicans* and reduce catheter colonization by about 16%.^[60] The use of silver-coated nylon fibres has been another area of research out of which the use of silvercel, which combines the use of a silver-coated nylon fibre with the enhanced exudate management properties of alginate fibres, is a paradigmatic example.^[61] Because of the sustained release of silver ions, the dressing acts as an effective barrier and helps reduce infection. Silvercel dressing has been proven effective *in vitro* against 150 clinically isolated microorganisms, including *C. albicans*.^[62]



Figure 7 - Cross section of catheter shows active release of silver ions from all catheter surfaces and into the surrounding environment, providing antimicrobial protection. (Retrieved from Oligon™)^[60]

The use of electrodeposition of ZnO nanoparticles or zinc -derived foams have also been proven to be efficient methods to alter the surface properties of biomaterials preventing colonization by *C. albicans* and/or *C. parapsilosis*. Marques *et al.* (2013) prepared zinc-derived foams that proved to be highly cytotoxic for *C. albicans* and with potential in inhibiting fungal cell growth.^[63] Alves *et al.* (2017) developed zinc oxide nanoparticle coatings that led to a reduction in the number of *C. parapsilosis* cells that colonized the surface. In turn, *C. albicans* cells were able to colonize between the zinc oxide crystals, leading to the detection of the superficial crystals and the effectiveness of the coating was compromised.^[64]

The use of chitosan matrixes incorporated with nanometallic components has also been used in dressings to prevent infections of wounds (Figure 8). The incorporation of metallic nanoparticles in the chitosan-based matrix favours sustained antimicrobial activity in proportion to matrix degradation without affecting the viability of normal cells. Although most studies performed the *in vitro* efficacy of these approaches in reducing growth of relevant infecting species, the toxicity posed by this chitosan-metallic nanoparticles *in vivo* remains to be addressed.^[65]

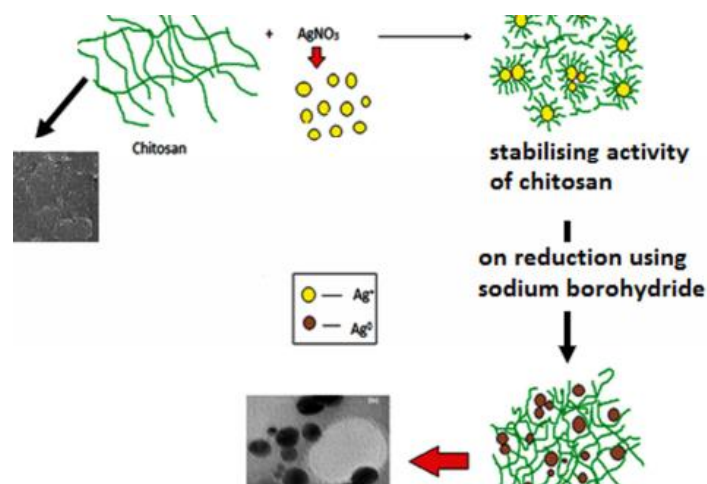


Figure 8 - Mechanism of formation of polymer matrix nanocomposite. In Nivethaa et al. (2015).^[65]

Other devices particularly susceptible to the establishment of biofilms by *Candida* species are intrauterine devices, IUDs. Taking this into account, Pippi et al. (2018) investigated the effect of clioquinol on preventing formation of *Candida* biofilms in these devices. Clioquinol is an antiseptic drug and is effective against multidrug-resistant *Candida*.^[66] The results showed that the coating of copper IUDs with clioquinol reduced by more than 80% the ability of *C. albicans* cells to form biofilms, which can be attributed essentially to blockage of hyphal development.^[66] These findings opened the door to a possible application of clioquinol in biomaterials, as it could be used as a coating to prevent morphological switching and thus prevent biofilm formation.

Generally speaking, the efficacy of these strategies is dictated by the potency of the combination of agents eluting and also by the maintenance of effective concentrations at the surfaces. An important aspect to mention is that the mechanisms underlying the antimicrobial activity of these approaches has not been clearly established and the results obtained until so far point to rather general mechanisms non-specifically targeting the bacterial or fungal cells, which might therefore represent an increased risk for toxicity against mammalian cells. It is thus essential to perform those type of determinations to render a more rational design of the strategies that can be implemented to reduce colonization of medical devices by important infecting species, including *Candida* spp.

1.5 Introduction to the theme of the thesis

New antifungal compounds focused on targets other than those used by conventional antifungals are urgently needed. Previous studies have shown that Ag(I) camphorimine complexes exhibit a high activity against *C. glabrata* and *C. parapsilosis* (the most effective drugs exhibited MICs of 15.6 µg/mL and 2.0 µg/mL, respectively), albeit this efficacy was found to be variable depending on the structure of the ligand.^[52] The fact that the more effective compounds were found to act in synergism with azoles and that they were able to sensitize azole-resistant strains^[67], further reinforces the interest in the study of these molecules as putative new anti-*Candida* agents. Despite this, none of the previously designed compounds showed the ability to sensitize *C. albicans*, this being attributable to the aptitude of these cells to mediate the formation of Ag nanoparticles^[52]. Another drawback attributable to the more effective Ag-camphorimine complexes developed is their high toxicity against mammalian cells (IC₅₀ of 0.05 mM), although it is important to point out that no significant cytotoxicity was observed for concentrations used synergistically with fluconazole. In this context, the first part of this thesis is focused on the synthesis of new coordination compounds using not only silver precursors other than silver nitrate, but as well as copper and zinc salts. The efficacy of these complexes in inhibiting the growth of *C. glabrata* and *C. albicans*, including some resistant clinical isolates of both strains, was also tested as well as the development of coatings for biomaterials exploring those compounds showing increased activity and at the same time low cytotoxic potential against mammalian cells. From a more academic perspective, the mechanisms underlying the resistance of two previously isolated resistant *C. albicans* clinical isolates were investigated in an attempt to contribute for the understanding of potential antifungal targets that could direct the design of new antifungals in future works.

2 Materials and methods

2.1 Synthesis and chemical characterization of the camphorimine complexes

2.1.1 Materials

Camphor and the appropriate amines were purchased from Sigma-Aldrich and Alfa Aesar, respectively. The precursors of coordination complexes were from Sigma-Aldrich and Acros Organic. The solvents (PA grade) were from Carlo Erba and Sigma-Aldrich.

2.1.2 Synthesis of Ligands

C₃₂H₃₆N₂O₂ (L1): (3,3)-3,3'-([1,1'-biphenyl]-4,4'-diylbis(azanylylidene))bis(1,7,7-trimethylbicyclo [2.2.1] heptan-2-one). Camphorquinone (330 mg; 2.0 mmol) was stirred in ethanol (6 mL) acidified with acetic acid (0.2 mL) at RT for 1 hour. Benzidine (184 mg; 1.0 mmol) was then added and the yellow mixture was stirred at 50°C for 21 hours. The solvent was removed under vacuum and the yellow solid was washed with diethyl ether and n-pentane. Yield 89%.

C₂₆H₃₂N₂O₂ (L2): (3,3)-3,3'-(1,4-phenylenebis(azanylylidene))bis(1,7,7-trimethylbicyclo[2.2.1] heptan-2-one). Camphorquinone (330 mg; 2.0 mmol) was stirred in ethanol (5 mL) acidified with acetic acid (0.17 mL) at RT for 20 minutes. *p*-phenylenediamine (106 mg; 1.0 mmol) was then added and the orange mixture was stirred at 50°C for 19 hours. After cooling, the solvent was removed under vacuum and the yellow solid was washed with n-pentane (3 x 5 mL). Yield 53%.

C₂₆H₃₂N₂O₂ L3: (3,3)-3,3'-(1,3-phenylenebis(azanylylidene))bis(1,7,7-trimethylbicyclo[2.2.1] heptan-2-one). Camphorquinone (310 mg; 1.9 mmol) was stirred in ethanol (5 mL) acidified with acetic acid (0.5 mL) at RT for 1 hour. *m*-Phenylenediamine (100 mg; 0.93 mmol) was then added and the mixture was stirred under nitrogen atmosphere at 50°C for 20 hours. By solvent removal, followed by addition of H₂O (4 mL) and extraction with CHCl₃ (3 x 5 mL) a solution was obtained that was dried over MgSO₄ for 2 hours. Upon filtration to separate the drying agent, the solvent was evaporated affording a yellow oil. Yield 66%.

A schematic representation of the ligands structures is shown in Figure 9 and the reactional schemes for the synthesized ligands is presented in Figure 10.

2.1.3 Synthesis of Complexes

The camphor derivatives and Cu(II) complexes were synthesized under air using conventional techniques and the Cu(I) complexes and Zn(II) complexes were synthesized under inert gas atmosphere using vacuum/Schlenk techniques. The Ag(I) complexes P, Q, R, S, T were synthesized by Joana Costa.^[52]

[CuCl₂(L1)]: (A)

CuCl₂·2H₂O (100 mg; 0.58 mmol) and ligand L1 (258 mg; 0.56 mmol) were mixed and THF (6 mL) was added and the solution was stirred for 1 hour at 40°C. The solvent was removed under vacuum and the brown solid dried. Yield 84%.

[CuCl₂(L3)]: (C)

CuCl₂·2H₂O (140 mg; 0.58 mmol) and ligand L3 (308 mg; 0.64 mmol) were mixed and THF (4 mL) was added. The solution was stirred for 1 hour at 40°C. The solvent was partially evaporated, and a green solid precipitated that was filtered and dried. Yield 54%.

[Cu(NO₃)₂(L1)]: (F)

Cu(NO₃)₂·3H₂O (70 mg; 0.29 mmol) and ligand L1 (156 mg; 0.32 mmol) were mixed and THF (4 mL) was added. The solution was stirred for 1 hour at 40°C. The solvent was partially evaporated and a green solid precipitated that was filtered, washed with ether (4 mL) and dried. Yield 81%.

[Cu(NO₃)₂(L3)]: (G)

Cu(NO₃)₂·3H₂O (70 mg; 0.29 mmol) and ligand L3 (156 mg; 0.32 mmol) were mixed and THF (4 mL) was added. The solution was stirred for 1 hour at 40°C. The solvent was partially evaporated until a green solid precipitated that was washed with ether (4 mL) and dried. Yield 97%.

[(CuCl)₂(L1)]: (I)

CuCl₂·2H₂O (79 mg; 0.79 mmol) and ligand L3 (190 mg; 0.40 mmol) were mixed and stayed under vacuum for 1h30. The solvent THF (3 mL) was added and the solution was stirred for 30 minutes at RT. The solvent was evaporated and the brown solid precipitated, that was washed with THF (4 mL) and dried under vacuum. The synthesis was made under inert gas atmosphere using vacuum/Schlenk techniques. Yield 57%.

[(CuCl)₂(L2)]: (J)

CuCl₂·2H₂O (100 mg; 1.01 mmol) and ligand L2 (204 mg; 0.51 mmol) were mixed and stayed under vacuum for 1h30. The solvent THF (5 mL) was added and the solution was stirred for 30 minutes at RT. The solvent was evaporated and the brown solid precipitated, that was washed with THF (4 mL) and dried under vacuum. The synthesis was made under inert gas atmosphere using vacuum/Schlenk techniques. Yield 62%.

[ZnCl₂(THF)(L1)] : (L)

ZnCl₂ (80 mg; 0.59 mmol) and ligand L1 (160 mg; 0.30 mmol) were mixed and THF (5 mL) was added and the solution was stirred for 3 hours at RT. The volume of the solvent was reduced and the orange solution was placed in the freezer overnight. The crystals obtained were filtered and dried. To the resulting solution it was added ether (1 mL). A precipitate formed that was discarded and the solution

was placed in the freezer overnight. Crystals formed that were filtered and the red solid was dried under vacuum. Yield 32%

2.1.4 Chemical characterization

FTIR spectra were obtained from KBr pellets using a JASCO FT/IR 4100 spectrometer. NMR spectra (^1H , ^{13}C , DEPT) were obtained from acetonitrile- d_3 (CD_3CN) or chloroform- d (CDCl_3) solutions using Bruker Avance II⁺ (400 MHz) spectrometer. NMR chemical shifts are referred to TMS ($\delta = 0$ ppm). Elemental analyses (C, N, H, S) were performed by Laboratório de Análises do Instituto Superior Técnico.

2.2 Strains and growth media used in the susceptibility assays

A cohort of *C. albicans* and *C. glabrata* clinical isolates recovered along epidemiological surveys undertaken in hospitals of the Lisbon area was used. ^[5,6] Besides these clinical isolates, the reference strains *C. albicans* SC5314 and *C. glabrata* CBS138 were used. The different strains were maintained at -80°C in YPD medium supplemented with 30% glycerol (v/v) (Merck). *Candida* cells were batch-cultured at 30°C , with orbital stirring (250 rpm) in rich growth medium Yeast Peptone Dextrose (YPD) or RPMI (Roswell Park Memorial Institute Medium). YPD contains, per liter, 20 g glucose (Merck Millipore), 10 g yeast extract (HiMedia Laboratories, Mumbai, India) and 20 g Peptone (HiMedia Laboratories). RPMI, contains, per liter 20.8 g RPMI-1640 synthetic medium (Sigma), 36 g glucose (Merck Millipore), 0.3 g of L-glutamine (Sigma) and 0.165 mol/L of MOPS (3-(N-morpholino) propanesulfonic acid, Sigma). All media were prepared in deionized water. YPD medium was sterilized by autoclave for 15 minutes at 121°C and 1 atm. RPMI medium was filtered with a $0.22\ \mu\text{m}$ pore size filter and preserved at 4°C until further use. Unless otherwise specified the pH of the RPMI growth medium was adjusted to 7.0 using NaOH as the alkalinizing agent.

2.2.1 Assessment of antifungal potential of the camphorimine complexes

The ability of the camphor-derived complexes to inhibit the growth of *Candida* species was assessed using the standardized microdilution method recommended by EUCAST (European Committee on Antimicrobial Susceptibility Testing) to determine the minimum inhibitory concentration (MIC) values, considered to be the concentration of drug that reduced yeast growth by more than 50% the growth registered in drug-free medium. Briefly, cells of the different species were cultivated at 30°C and with 250 rpm orbital agitation for 18h in YPD growth medium and then diluted in fresh RPMI growth medium (Sigma) to obtain a cell suspension having an $\text{OD}_{600\text{nm}}$ of 0.05. From these cell suspensions, $100\ \mu\text{L}$ aliquots were mixed in the 96-multiwell polystyrene plates with $100\ \mu\text{L}$ of fresh RPMI medium (control) or with $100\ \mu\text{L}$ of this same medium supplemented with 0.98, 1.95, 3.91, 7.81, 15.63, 31.25, 62.5, 125.0, 250.0, 500.0 $\mu\text{g/mL}$ of the different compounds. The stock solutions of Ag(I)-derived compounds were

prepared from the powder, using DMSO (Dimethyl sulfoxide, Sigma) as the solvent. As a control was also examined the inhibitory effect of precursors and free ligands. After inoculation, the 96-multiwell plates were incubated without agitation at 37°C for 24h. After that time, cells were resuspended and the OD_{530nm} of the cultures was measured in a microplate reader. The MIC value was taken as being the lowest concentration tested at which the growth of the strains was 50% of the value registered in the control lane.

2.2.2 Assessment of synergistic effect of Ag(I) camphorimine complexes with fluconazole in *C. albicans*

The existence of a synergistic effect between the Ag(I)-based camphorimine complexes and fluconazole was tested using a checkerboard method [52] in which the MIC for the different drugs (alone or in combination) is determined using a microdilution method similar to the one described in 2.3. The MIC value determined was afterwards used to calculate the fractional inhibitory concentration index (FICI), through the following formula: $\Sigma FICI = FICA + FICB$, where $FICA = MIC_{A \text{ in combination}} / MIC_A$ alone, and $FICB = MIC_{B \text{ in combination}} / MIC_B$ alone. FICI values ≤ 0.5 indicate synergism; between 0.5–4.0, no interaction; > 4.0 , antagonism. The concentrations used for each chemical agent was: for the Ag(I)-based camphorimine complexes 0.063 and 0.125 $\mu\text{g/mL}$, for fluconazole, 0.98 and 1.95 $\mu\text{g/mL}$.

2.2.3 Coating functionalization of stainless steel plates with Ag(I)-camphorimine complexes

The polycaprolactone (PCL) solutions were prepared at concentrations of 8% and 4% (w/v) using TFA (Trifluoroacetic acid, Sigma), chloroform (Carl Roth) or dichloromethane (Carl Roth) as solvents. PCL pellets (Sigma) were dissolved for 3 hours in magnetic stirrer at room temperature. For the PCL coating preparation, 316L stainless steel (SS) plates were previously polished with grit P600 and P1200 to ensure a homogeneous surface pattern and then submerged in acetone (Sigma) prior to dip-coating process to wash out any impurity. Dip-coating was done on PCL solutions without and with compounds P or Q. The stock solutions of Ag(I)-derived compounds were prepared from the powder, using DMSO (Dimethyl sulfoxide, Sigma) as the solvent. PCL solutions were prepared with compound P at concentrations of 0.156 $\mu\text{g/mL}$ and 1.56 $\mu\text{g/mL}$ (P10 and P100, respectively) and with compound Q at concentrations 0.313 $\mu\text{g/mL}$ and 3.13 $\mu\text{g/mL}$ (Q10 and Q100, respectively). The dipping process was made by using Siemens Logo 12/24 RC and consisted of the complete dip of the SS plates, which were removed from the dip-coating solution at a speed of 0.3 $\text{cm}\cdot\text{s}^{-1}$. After 1 minute drying a second dip was made using the same conditions, after which the plates dried overnight at RT.

2.2.3.1 Physical-chemical characterization of the surfaces

The morphological and chemical characterization of the isolated compounds and of the newly synthesized coatings were analyzed by scanning electron microscopy (SEM) using a JEOL-JSM7001F

or Hitachi S2400 apparatus and the elemental chemical composition by the respective X-ray energy dispersion spectrometer (EDS). To increase the conductivity of the samples, a conductive thin layer of gold and palladium was applied with a Polaron E-5100.

2.2.3.2 Assessment of the effect of PCL coatings on the ability of *C. albicans* to form biofilms on the surface of stainless steel plates

The ability of *C. albicans* SC5314 to form biofilms on bare or coated SS surfaces was tested using an experimental setup used previously with success.^[65] Cells were cultivated at 30°C with orbital agitation in rich YPD growth medium until mid-exponential phase ($OD_{600nm}=1\pm 0.1$) and then re-inoculated (at an initial OD_{600nm} of 0.1 ± 0.01) in a 25 mL capacity beaker containing 4.5 mL of fresh RPMI growth medium (Sigma) at pH 7. After inoculation, bare or coated plates were submerged in the prepared cell suspension. The cultures were grown at 37 °C with gentle shaking (30 rpm) for 48 h. After this time, bare or coated plates were removed and washed twice with distilled water to eliminate non-adherent cells. The number of viable cells adhered to the surfaces was quantified after washing the plates with distilled water and scratching the surface to remove the adhered cells. The scratched material was diluted in 1 mL of sterile distilled water and serial dilutions were subsequently performed (in a range of 10^{-1} to 10^{-4}). Fifty microliters of each cell suspension were plated on solid YPD growth medium and the number of colony forming units (CFUs) formed 48 hours after incubation, at 30°C, was quantified. The number of CFUs present in the supernatant was also determined. For this, 1 mL of each supernatant was diluted (1:10) in sterile water after which serial dilutions (in a range of 10^{-1} to 10^{-5}) were subsequently prepared and fifty microliters of each cell suspension were plated on solid YPD growth medium. For the observation of the biofilms formed on the surface of bare or coated surfaces, plates were washed with distilled water, and immersed in 70 % (v/v) ethanol for 10 min, with 95 % (v/v) ethanol for 10 min and finally with absolute ethanol for 20 min to fix cells to the surface. After complete air-drying, the plates were coated with a conductive thin layer of gold and palladium applied with a Polaron E-5100 and analyzed by SEM (JEOL-JSM7001F or Hitachi S2400).

2.2.4 Determination of MICs to fluconazole

To assess the resistance phenotype of strains *C. albicans* 10A and 22CL and of the reference strain SC5314 to fluconazole, the MIC was estimated using the microdilution method recommended by EUCAST.^[9] The concentrations of fluconazole tested ranged from 0.125 to 128 µg/mL. The MIC determined for the strains was compared with the clinical breakpoints recommended by EUCAST (4 µg/mL for fluconazole for *C. albicans*) to classify the strains as resistant (the MIC determined is above the defined breakpoint) or susceptible (MIC equal or below the breakpoint). The stock solutions of the antifungal were prepared from the powder, using DMSO (dimethyl sulfoxide, Sigma) as the solvent and fluconazole was purchased from Sigma and the microdilution assay protocol followed was similar to those described above in 2.3. To perform microscopic observations of the cells cultivated after 24h under these conditions, the cells diluted 1:2 in sterile water and observed in a light microscope using a 100x magnification lens. To assess viability of the cells under these conditions serial dilutions (using

Phosphate Buffered Saline (PBS) as a solvent) of the cellular suspensions were performed (in a range of 10^{-1} to 10^{-6}) and fifty microliters of these plated on solid YPD growth medium. The number of colonies formed after 48 hours after incubation of the plates at 30°C was taken as a measure of viability. To accompany the growth curve of the strains in the presence of fluconazole under the above described experimental conditions, the same setup was used with the difference that instead of taking a single time point in the OD of the culture (taken after 24 h), readings were performed every 6 hours, during 120 h.

2.2.5 Qualitative assessment of the FoG population in isolates 10A, 22CL and SC5314

To make a qualitative assessment of the fraction of cells (FoG) that grow in the presence of fluconazole (composing so called tolerant population) a disk diffusion assay was used. For that, the standardized method recommended by the EUCAST was used. Briefly, 85 mm diameter Petri dishes (with 4 mm thickness) supplemented with 25 µg of fluconazole were placed on the top of MHB plates. Cells from different isolates were grown overnight at 30°C for 24 hours in 5 mL of liquid YPD. The following day this pre-inoculum was used to prepare a cell suspension (using sterile water as solvent) with an OD_{600nm} of 0.05 and 50 µL of this cell suspension was spread on the Petri dishes prepared and the discs with fluconazole were then placed. Images were obtained after 48h of incubation at 37°C.

3 Results and Discussion

3.1 “Re-design” of Ag(I)-based camphorimine complexes and assessment of their anti-*Candida* potential

One of the goals of this work was to redesign previously used camphor derived ligands to get Ag(I)-camphorimine complexes with improved anti-*Candida* potential (extending it to *C. albicans*), while minimizing their cytotoxic potential against mammalian cells. To do so, silver nitrate (that was used as a precursor before) was replaced for silver chloride AgCl and silver hydroxide Ag(OAc). This work was based on the synthesis of camphorimine ligands that were chosen based on previous results that showed that these were convenient ligands for biologically-active complexes, since these had suitable structural and electronic characteristics.^[52] The camphorimine ligands were synthesized under air using conventional organic synthesis techniques. A schematic representation of the ligands structures is shown in Figure 9 and the reactional schemes for the synthesized ligands is presented in Figure 10.

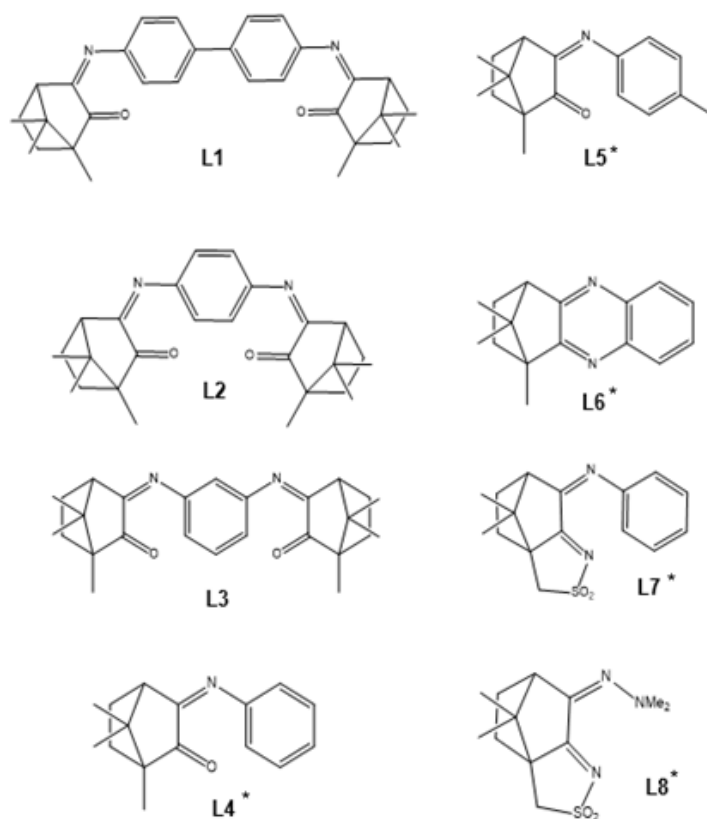


Figure 9 - Camphorimine (L1-L6) and camphor-sulfonylimine (L7,L8) derivatives used as ligands. Ligands marked with * were synthesized by Joana Costa.

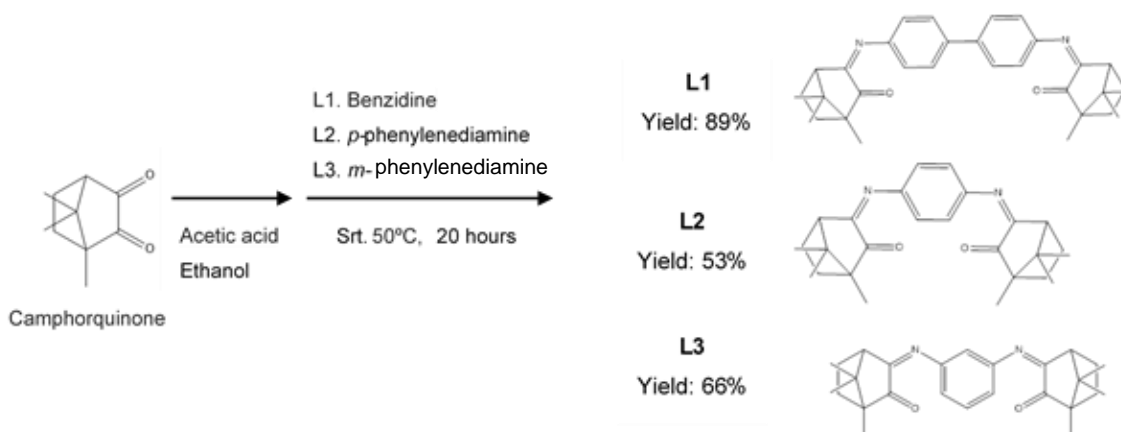


Figure 10 - Reactional schemes for the synthesized ligands: L1, L2 and L3.

Silver complexes were then synthesized under an inert gas atmosphere using vacuum/Schlenk techniques. The characterization of the ligands and complexes was based on elemental analysis, Fourier Transform Infrared spectroscopy (FTIR) and Nuclear Magnetic Resonance (NMR). The FTIR and NMR (^1H , ^{13}C) spectra allowed the ready identification and attribution of the C=O and C=N groups in the new molecules and formulate a hypothetical chemical formula of the novel compounds, which is then corroborated by elemental analysis. ^1H NMR detects each analyte proton and the integration curve for each proton reflects the abundance of the individual protons, while ^{13}C NMR allows the identification of carbon atoms in an organic molecule. As an example, the information provided by FTIR and NMR (^1H , ^{13}C) spectra obtained for compound P (Table iv) is shown in Figures 11, 12 and 13, respectively.

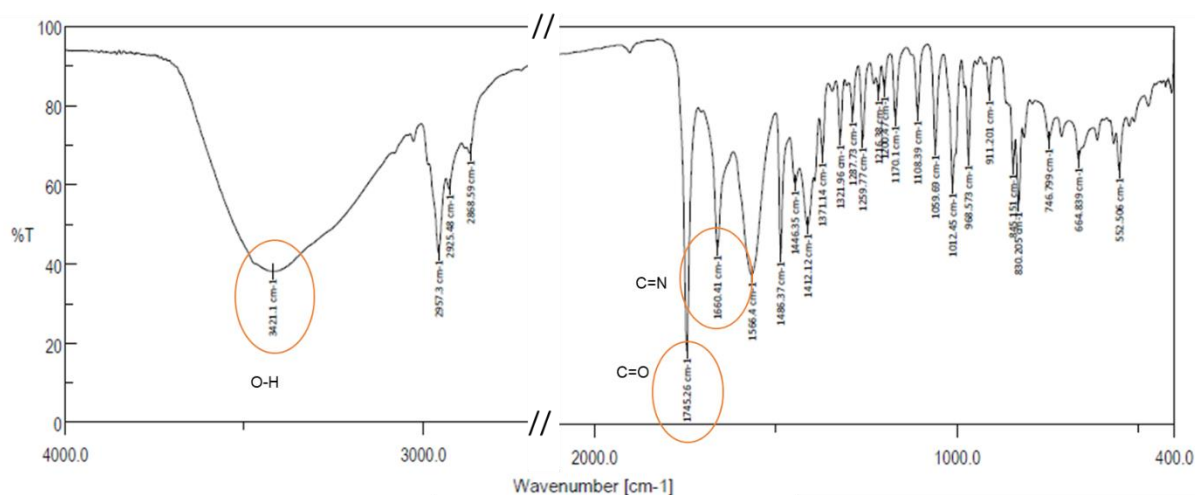


Figure 11 - FTIR spectrum of complex P, showing bands respective to O-H, C=O and C=N bonds.

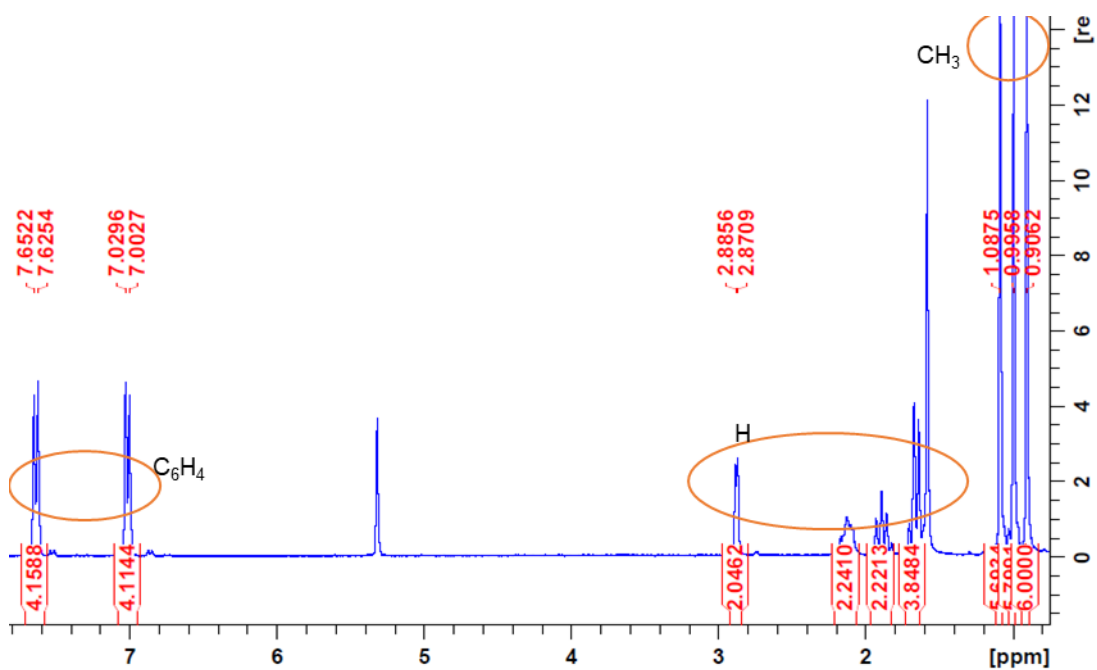


Figure 12 - ¹H NMR spectrum of complex P (detailed characterization in experimental section), showing the characteristic chemical shifts of the hydrogen atoms respective to the C₆H₄, H and CH₃ groups..

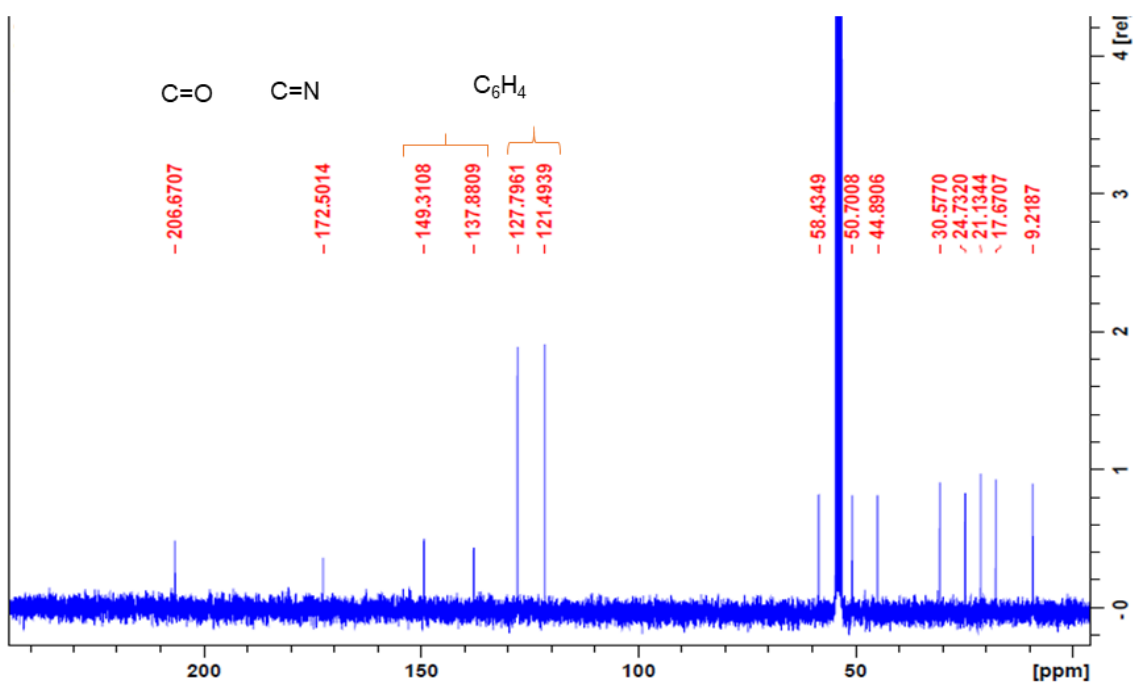


Figure 13 - ¹³C NMR spectrum of complex P (detailed characterization in experimental section), showing the characteristic chemical shifts of the several carbon atoms.

The anti-*Candida* potential of the ligands and precursors used and of the resulting silver-containing complexes was determined based on quantification of MIC (the concentration of drug that inhibits growth by more than 50%, comparing with growth observed in drug-free medium) against the reference species *C. albicans* SC5314 and *C. glabrata* CBS138. An example of the results that were obtained in this assay and that allowed the estimation of MIC is shown in Figure 14, which corresponds to the results obtained for the most effective compound, compound P (all other results obtained are presented in Annexes – Figures 31, 32) and the detailed set of MICs obtained is shown in Table iii. Note that at concentrations of 250 and 500 µg/mL, precipitation of the compound may occur and growth increases.

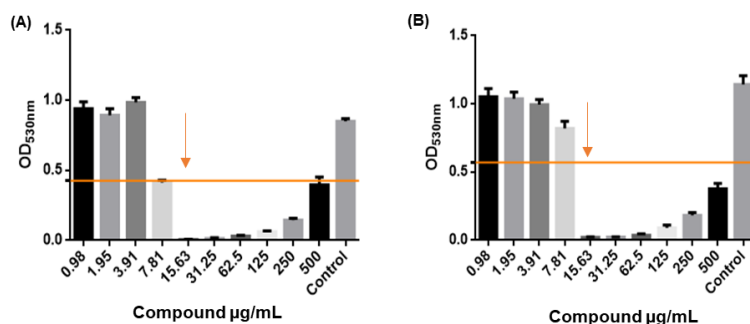


Figure 14 - Microdilution assay for complex P against the reference species (A) *C. albicans* SC5314 and (B) *C. glabrata* CBS138. The MIC value is indicated by an orange arrow and the 50% reduction of the growth registered in the absence of the chemicals is indicated by the orange line.

Table iii - MIC values (µg/mL) of the ligands, precursors and silver complexes against *C. albicans* (SC5314) and *C. glabrata* (CBS138), based on the EUCAST microdilution method. The complexes P, Q, R, S and T were synthesized by someone else.

Precursor	Ligand	Compound formula	Abbreviation	MIC (µg/mL)	
				<i>C. albicans</i>	<i>C. glabrata</i>
-	L1	-	--	>500	>500
-	L2	-	-	>500	>500
-	L3	-	-	>500	>500
Ag(OAc)	-	-	-	>500	>500
	L1	[Ag(OH)L1]	P	15.63	15.63
	L5	[[Ag(L5)] ₂ (µ-O)]	Q	31.25	31.25
	L6	[[Ag(OH)] ₂ L6]	R	62.50	125
AgCl	-	-	-	>500	>500
	L4	[(AgCl)L4]	S	250	250

	L5	$[\{Ag(L5)\}_2(\mu-O)]$	T	250	>500
--	----	-------------------------	---	-----	------

Based on the results presented in Table iii, it is verified that within the range of concentrations tested, none of the ligands exhibited activity against the two *Candida* species tested, as well as the precursors used, namely Ag(OAc) and AgCl, while the silver complexes were quite effective against these yeasts. Nevertheless, the most promising results were found for the coordination complexes having Ag(OAc) as precursor, once the MIC values obtained were quite low against both *C. albicans* and *C. glabrata* (Table iii). With this result, it can be said that one of the initial objectives of this thesis was reached, since it was possible to identify alternatives to the previously used Ag(I)-camphorimine complexes to reach sensitization of *C. albicans*.^[52] In the work of Cardoso (2017) *et al.*^[52], the ability of this species to catalyze the formation of silver nanoparticles on the cell's surface was reported (presumably due to very small amounts of silver nitrate present in the mixture and that could serve as reducing agents for the formation of silver nanoparticles) and this characteristic is likely to be the basis of activity against *C. albicans*. Here, using a different precursor in the synthesis of these complexes it was possible to obtain new compounds with higher antifungal potential and greater spectrum of antifungal action. Regarding *C. glabrata*, the MIC values obtained were like the ones reported by Cardoso (2017) *et al.*^[52], in the range of 15.63 to 125 µg/mL.

3.2 Synthesis of ligands and of Zn- and Cu- based complexes and assessment of their anti-*Candida* potential

In an attempt to design new, cheaper and effective antifungal compounds, camphorimine ligands were used to coordinate copper and zinc to generate Cu(I), Cu(II) and Zn(II) coordination complexes. The choice of using zinc and copper to synthesize new complexes and assess their anti-*Candida* potential was based on the well-known biocompatibility of these metals, along with relevant roles as immunomodulators and antimicrobial potential.^[56] The precursors of Cu(II) coordination complexes used were $CuCl_2 \cdot 2H_2O$ and $Cu(NO_3)_2 \cdot 3H_2O$, while for Cu(I) coordination complexes it was used CuCl, and for Zn(II) coordination complexes, $ZnCl_2$. The Cu(II) complexes were synthesized under air using conventional organic synthesis techniques, while Cu(I) and Zn(II) complexes were synthesized under an inert gas atmosphere using vacuum/Schlenk techniques (Table iv). The reactional schemes for the synthesized complexes are presented in Figure 15.

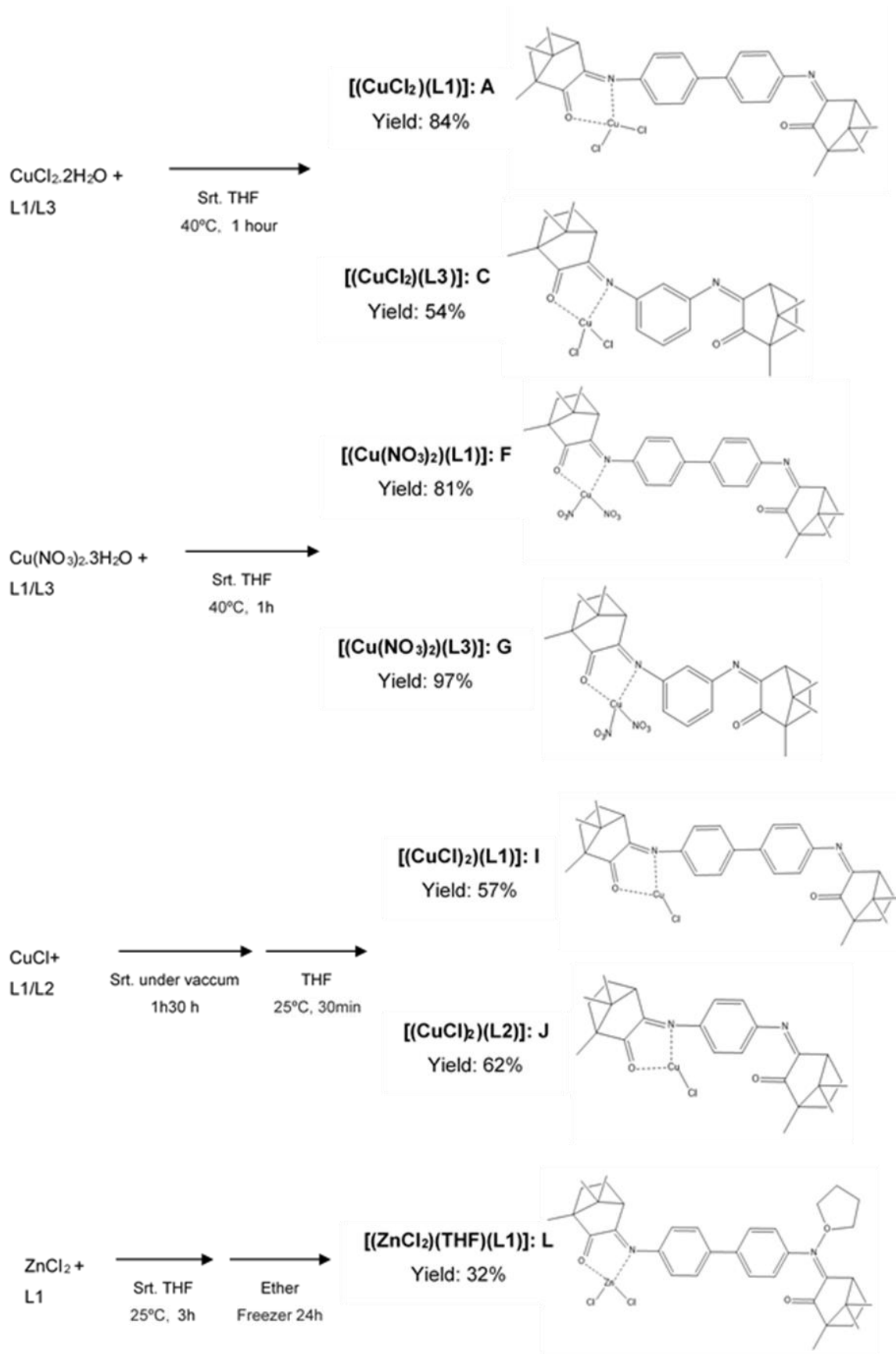


Figure 15 - Reactional schemes for the synthesized complexes of Cu(II), Cu(I) and Zn(II).

The characterization of the complexes was based on elemental analysis, Fourier Transform Infrared spectroscopy (FTIR) and Nuclear Magnetic Resonance (NMR), with the exception of Cu(II) complexes, because it was not possible to obtain NMR spectrum for this element due to its paramagnetic character. In addition, it was also not possible to obtain NMR spectra for the complexes of Cu(I) and Zn(II), due to decomposition during acquisition. Detailed characterization is presented in experimental section. The anti-*Candida* potential of the precursors used as well as of the seven synthesized complexes (molecules A, C, F, G, I, J, L in Table iv) and of the seven copper- or zinc- containing complexes that were already available in the CQE laboratory (B, D, E, K, M, N, O in Table iv) was determined against *C. albicans* SC5314 and *C. glabrata* CBS138. All the results that were obtained in this assay and that allowed the estimation of MIC are presented in Annexes – Figures 31, 32 and the detailed set of MICs obtained is shown in Table iv.

Table iv - MIC values ($\mu\text{g/mL}$) of the precursors and copper and zinc complexes against *C. albicans* (SC5314) and *C. glabrata* (CBS138), based on the EUCAST microdilution method. The complexes B, D, E, K, M, N and O were not synthesized during the course of this work and were already available in the CQE laboratory.

Precursor	Ligand	Compound formula	Abbreviation	MIC ($\mu\text{g/mL}$)	
				<i>C. albicans</i> SC5314	<i>C. glabrata</i> CBS138
CuCl ₂ ·2H ₂ O	-	-	-	>500	>500
	L1	[(CuCl ₂)(L1)]	A	>500	125
	L2	[(CuCl ₂)(L2)]*	B	>500	>500
	L3	[(CuCl ₂)(L3)]	C	>500	>500
	L6	[(CuCl ₂)(L6)]*	D	>500	62.50
	L7	[(CuCl ₂)(L7)]*	E	>500	125
Cu(NO ₃) ₂ ·3H ₂ O	-	-	-	>500	62.50
	L1	[(Cu(NO ₃) ₂)(L1)]	F	>500	125
	L3	[(Cu(NO ₃) ₂)(L3)]	G	>500	>500
CuCl	-	-	-	>500	31.25
	L1	[(CuCl) ₂ (L1)]	I	>500	125
	L2	[(CuCl) ₂ (L2)]	J	>500	>500
	L6	[(CuCl) ₂ (L6)]*	K	250	31.25
-	-	-	-	>500	>500

ZnCl₂	L1	[(ZnCl ₂)(THF)(L1)]	L	>500	>500
	L2	[(ZnCl ₂)(THF)(L2)]*	M	>500	>500
	L3	[(ZnCl ₂)(THF)(L3)]*	N	>500	>500
	L8	[(ZnCl ₂)(THF)(L8)]*	O	>500	>500

Within the range of concentrations tested, CuCl₂·2H₂O used as a precursor in synthesis of A, B, C, D and E exhibited no activity against the two *Candida* species tested. Concerning Cu(NO₃)₂·3H₂O and CuCl, precursors of F, G and I, J, K, respectively, no significant activity was registered against *C. albicans*, however, *C. glabrata* was found to be quite sensitive showing MIC values that were even below those obtained with some of the complexes synthesized from this precursor.

With the exception of the K complex, none of the other Zn- or Cu- containing complexes tested showed activity against *C. albicans* (Table iv). In the case of *C. glabrata*, the Cu(II) complexes A, D, E and F exhibited activity, although a higher efficacy seems to be achieved using Cu(I) complexes (e.g. compare molecules D and K that have the same ligands differing only in the precursors).

An interesting aspect is that the Cu(II)- or Cu(I)- complexes more active were those having the L1 and L6 ligands (Table iv). These results demonstrate the importance that the ligands have in the complex formed, since complexes with the same metal center behave differently depending on the coordinated ligands and how they influence the structure of the molecule. The characteristics of the final molecule will determine its ability to interact with *Candida* cells and to inhibit their growth.

Concerning the zinc-containing complexes, for none of them was observed efficacy against neither of the species tested. Although the same ligands were used as in the previous complexes, zinc appears to have less obvious effects. On the one hand, in the zinc reactions low yields were obtained, indicating that the reactions may not have been complete and the complex molecules would be few in the final product. On the other hand, zinc does not appear to be as effective as antifungal as silver.^[68] It is possible that conjugation in a complex inhibits its action, but further studies are needed to evaluate the mechanism of action of these molecules in the cell and thus understand why they were not effective.

When comparing the silver complexes with the above copper and zinc complexes, Ag(I)-camphorimine complexes are undoubtedly the most promising. It should be noted that the complex with the highest activity is P, whose ligand is L1. Previously, for the copper complexes it was also found that the most effective complexes were coordinated with L1, namely complexes A, F and I (Table iv). This evidence indicates that this ligand presents characteristics that allow the complex to interact in some way with *Candida* cells and somehow inhibit their growth. In the future, it will be interesting to explore the mechanism of action of these most active complexes and how they interact with cells and condition their growth.

3.3 Ability of Ag(I)-based camphorimine complexes to act against azole-resistant *Candida* strains and its synergistic effect with fluconazole

Based on the results obtained it was decided to further proceed with the study of compounds P and Q (Table iii) since they exhibited the high efficacy against both *C. albicans* and *C. glabrata*. In order to confirm whether these compounds would also be able to act against clinical isolates of *C. albicans* and *C. glabrata*, including those exhibiting resistance to fluconazole, a set of 10 strains available in the laboratory (2 *C. albicans* strains, 10A and 22CL, and 8 *C. glabrata* strains, FFUL29, FFUL412, FFUL443, FFUL830, FFUL866, FFUL874, 8estef and 36estef) were phenotyped for their tolerance to P and Q.^[69,70] The results obtained are summarized in Fig. 16 and presented in a more detailed form in Figure 17 for *C. albicans* strains and in Annexes – Figures 33, 34 for *C. glabrata* strains.

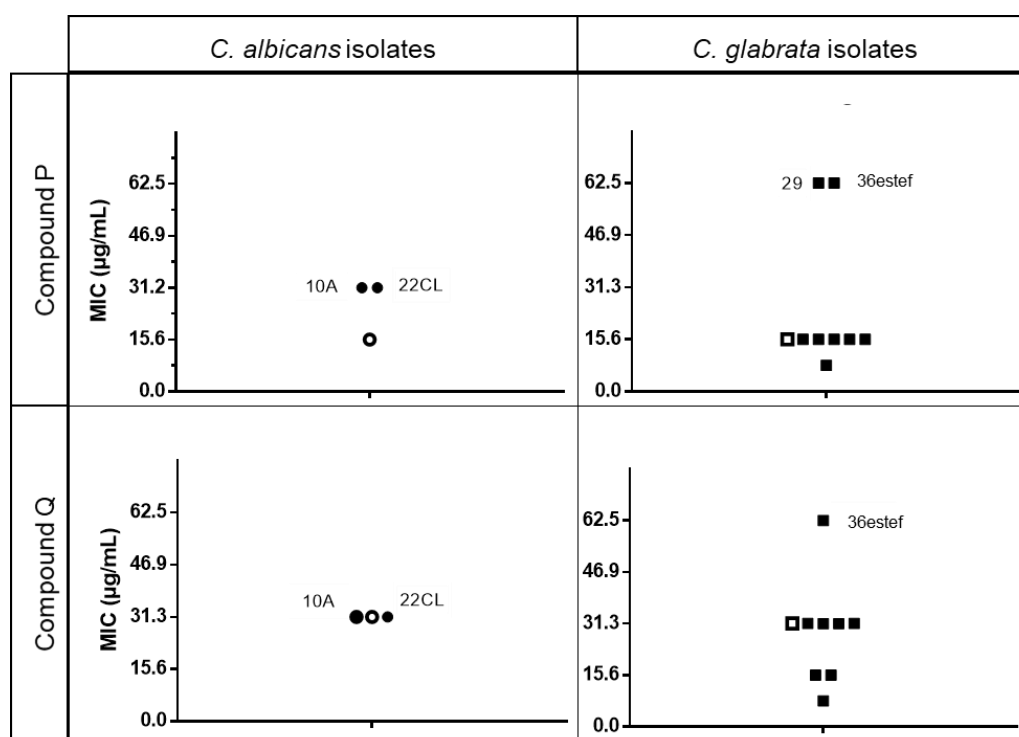


Figure 16 - MIC values ($\mu\text{g/mL}$) of the complexes P and Q, obtained for the reference *C. albicans* (SC5314) strain and respective isolates, represented by \bullet , and for the reference *C. glabrata* (CBS138) strain and respective isolates, represented by \blacksquare . The reference strains are represented by empty symbols. The most tolerant strains have the highlighted name.

The results obtained confirmed that the Ag-containing complexes were able to act against the clinical isolates to a level similar to the one obtained for the reference strains, although in the case of *C. glabrata* there were some strain-dependent effect with the 36estef strain showing higher tolerance to both P and Q. This ability suggests that these complexes should have biological targets other than those targeted by azoles, which is a highly desirable trait. A surprising aspect of the growth profile performed was the fact that the *C. albicans* isolates grew better in the presence of the lower concentrations of the

compounds tested (1.95, 3.91 and 7.81 $\mu\text{g/mL}$ concentrations) than in control conditions (Figure 17). We have confirmed that this is indeed higher growth since the number of CFUs/mL was higher in the presence of the low concentrations of P and Q than in control conditions. Further studies will be required to understand these observations.

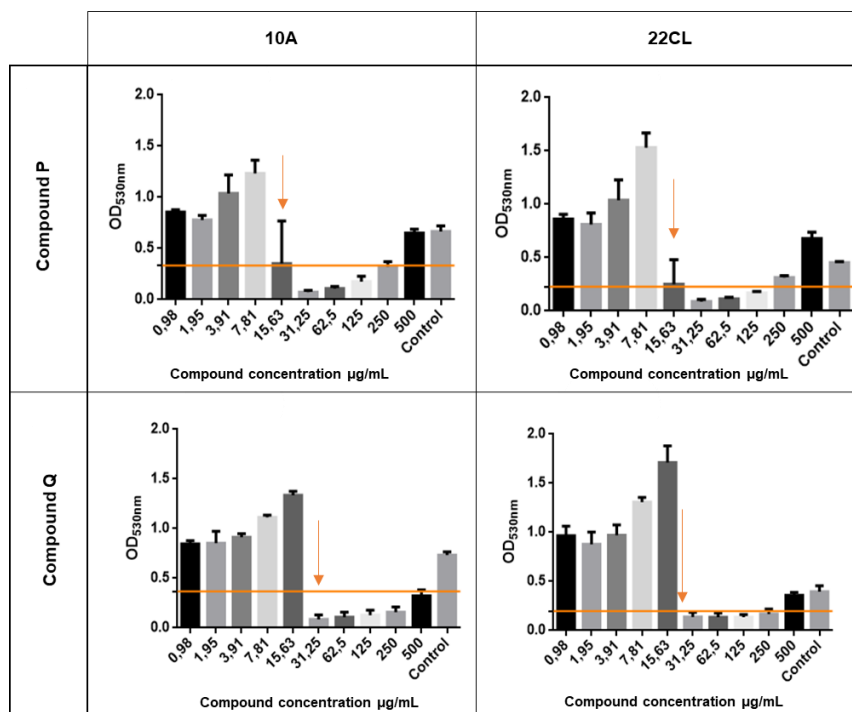


Figure 17 - Microdilution assay for all the complexes P and Q against the azole resistant isolates of *C. albicans* 10A and 22CL. The MIC value is indicated by an orange arrow and the 50% reduction of the growth registered in the absence of the chemicals is indicated by the orange line

The next step of this work was to determine whether the previously observed synergistic effect of Ag(I)-camphorimine complexes with fluconazole in *C. glabrata* [67] could also be observed for these new complexes. Fluconazole is one of the most used antifungal drugs in the clinical practice and an interesting strategy to improve susceptibility of *Candida* cells to this type of drugs could be through its application in synergism with other sensitizing chemicals. This strategy has already been confirmed in other trials for *C. glabrata* with complexes synthesized from precursors different from those used in this work.[67] However, it was not known whether this effect also occurred with *C. albicans*. The possibility of a synergistic effect between the Ag(I)-camphorimine compounds P and Q with fluconazole was evaluated against the reference strain *C. albicans* SC5314 but also against the resistant isolates 10A and 22CL.

For this, the *C. albicans* cells were cultivated in the presence of two non-inhibitory concentrations of the coordination complexes P and Q (0.98 $\mu\text{g/mL}$ and 1.95 $\mu\text{g/mL}$), selected based on the results obtained in the previous tests (Annexes – Figure 35), or combined with two non-inhibitory concentrations of fluconazole, 0.063 $\mu\text{g/mL}$ and 0.125 $\mu\text{g/mL}$. In Figure 18 are represented the heatmaps obtained in the synergism assay of the reference strain SC5314 and the two azole-resistant

clinical isolates, 10A and 22CL. To have a clearer view of the data obtained, in Annex – Figure 35 is shown the optical density of the cultures obtained after 24h of growth in the different conditions. The results obtained could not confirm a synergistic effect between complexes P and Q with fluconazole since the fractional inhibitory concentration index (FICI) (calculated following the formula: $\Sigma FICI = FICA + FICB$, where $FICA = MICA \text{ in combination} / MICA \text{ alone}$, and $FICB = MICB \text{ in combination} / MICB \text{ alone}$) obtained and present in Figure 18 indicated no interaction. This result is, somehow, in line with the lack of similarity of targets for these two groups of molecules, although, it could be helpful to repeat this assay using higher non-inhibitory concentrations of the complexes than those tested here.

SC5413		FLC (µg/mL)		
		0	0.063	0.125
Compound P (µg/mL)	0			
	0.98			
	1.95			
FICI		1.7		

SC5413		FLC (µg/mL)		
		0	0.063	0.125
Compound Q (µg/mL)	0			
	0.98			
	1.95			
FICI		2.1		

10A		FLC (µg/mL)		
		0	0.063	0.125
Compound P (µg/mL)	0			
	0.98			
	1.95			
FICI		2.1		

10A		FLC (µg/mL)		
		0	0.063	0.125
Compound Q (µg/mL)	0			
	0.98			
	1.95			
FICI		2.3		

22CL		FLC (µg/mL)		
		0	0.063	0.125
Compound P (µg/mL)	0			
	0.98			
	1.95			
FICI		1.5		

22CL		FLC (µg/mL)		
		0	0.063	0.125
Compound Q (µg/mL)	0			
	0.98			
	1.95			
FICI		1.9		

Figure 18 - Heatmaps obtained in the synergism assay used to assess the potential of the synergistic effect of fluconazole and camphorimine compounds P and Q against the reference strain for *C. albicans* (SC5314) and resistant isolates of the same strain, 10A and 22CL. Dark green corresponds to a higher and dark red to reduced growth. FICI correspond to the fractional inhibitory concentration index and the values calculated indicate no interaction.

3.4 Using Ag(I)-based camphorimine complexes in the design of new coatings for functionalizing medically relevant surfaces

Considering the results obtained for the activity of compounds P and Q in inhibiting growth of *Candida albicans* and *Candida glabrata*, the next step was to try to apply these molecules as coatings of surfaces. To get a better characterization of the compounds P and Q, a deeper physicochemical analysis of these compounds was performed by scanning electron microscopy (SEM) and elemental chemical composition by X-ray energy dispersive spectrometry (EDS).

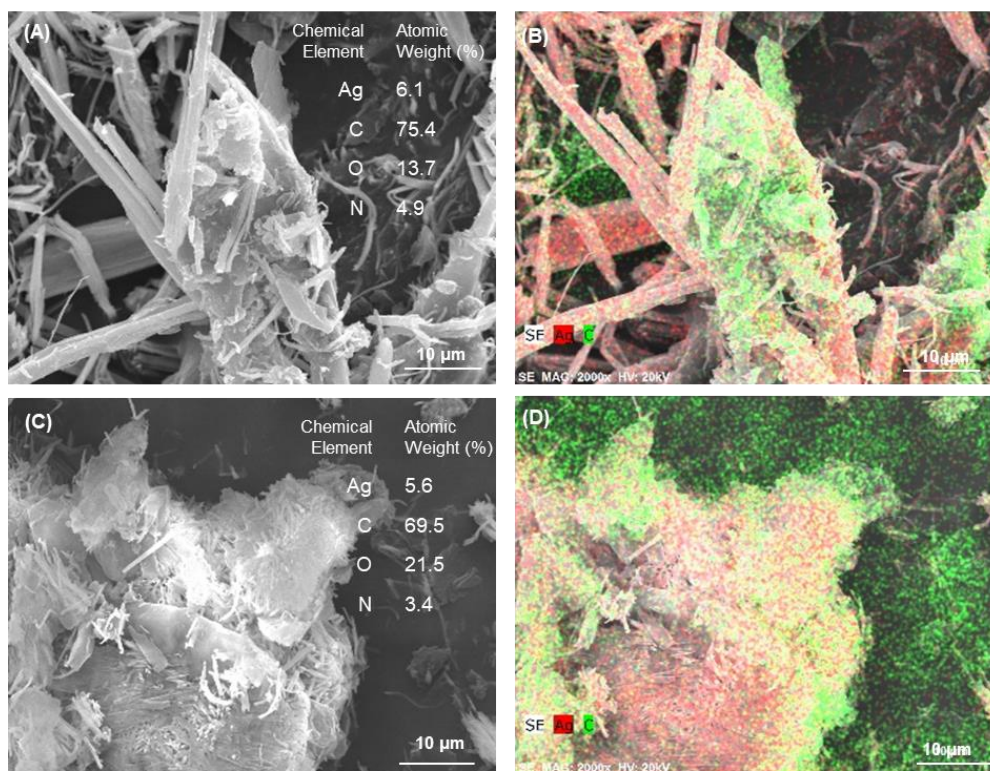


Figure 19 - Scanning electron microscopy (SEM) micrographs for (A, C) and corresponding X-ray energy dispersive spectrometer (EDS) maps (B, D) for compound P (A, B) and compound Q (C, D) in powder; In EDS maps silver (Ag) is marked in red and carbon (C) in green.

Despite the different morphology, the presence of silver was confirmed in both compounds (Figure 19). Compound P was composed by needles, where silver was concentrated, and blocks where this element was not detected, as shown in Figure 19 (A, B). In the compound Q silver was detected in different structures, being present in large aggregates (C, D).

The strategy used to immobilize these compounds (P and Q) on a biomaterial surface started by choosing which was the best methodology to vehicle them. We started to test their incorporation in biodegradable polymeric coatings used in 316L stainless steel sheets, used in medical implants and prostheses.^[70] Polycaprolactone (PCL), a polyester, was selected as the first polymer to be tested.^[71] An appropriate solvent also had to be selected aiming to solubilize the compounds P and Q and also

PCL. Trifluoroacetic acid (TFA), chloroform and dichloromethane were tested for that purpose (Figure 20).




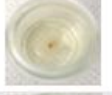


	Compound P	Compound Q
Trifluoroacetic acid (TFA)	+ 	+ 
Chloroform	+ 	- 
Dichloromethane	- 	- 

Figure 20 - Solubility of compounds P and Q in trifluoroacetic acid (TFA), chloroform and dichloromethane. Complete dissolution (+) and incomplete dissolution with precipitate formation (-).

Initially, PCL coatings were formulated using TFA as a solvent and an 8% (w/v) polymer concentration. After drying, the coating broke off from the stainless steel (SS) surface (Figure 21 A-C). Following this result and since TFA releases toxic gases that can cause severe skin burns [72], it was decided to use chloroform and 8% (w/v) PCL. Once again, the coating broke and was detached from the SS surface after drying (Figure 21 D-F). According to the elemental chemical composition by the respective X-ray energy dispersive spectrometer (EDS), the contents of C and O were about 80% and 20% for coatings using TFA and 83% and 17% for coating using chloroform, respectively (Atomic Weight %). Despite using the same PCL percentage, this difference in C and O contents may be related with solvents promoting different molecular arrangements of the polymer.

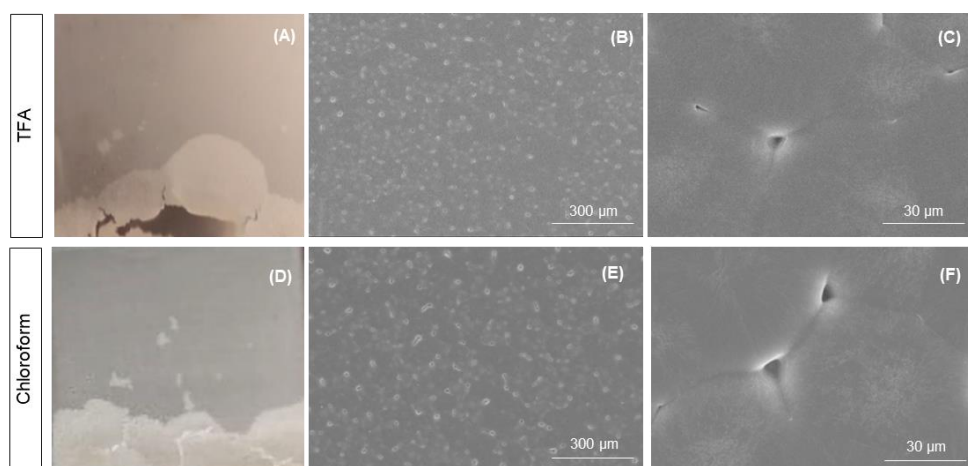


Figure 21 - Photographs of PCL 8% broken coatings using TFA (A) and chloroform (D) as solvents. Scanning electron microscopy (SEM) micrographs of PCL 8% coatings using TFA (B,C) and chloroform (E, F) as solvents.

Given that the coating broke in the previous tests, PCL concentration was reduced to 4% (w/v). As can be seen in Figure 22, the dried coatings using both chloroform (Figure 22 A-C) or dichloromethane (Figure 22 D-F) as solvents remained intact. As reported by the elemental chemical composition from EDS, the contents of C and O were about 85% and 15% for both coatings (Atomic Weight %).

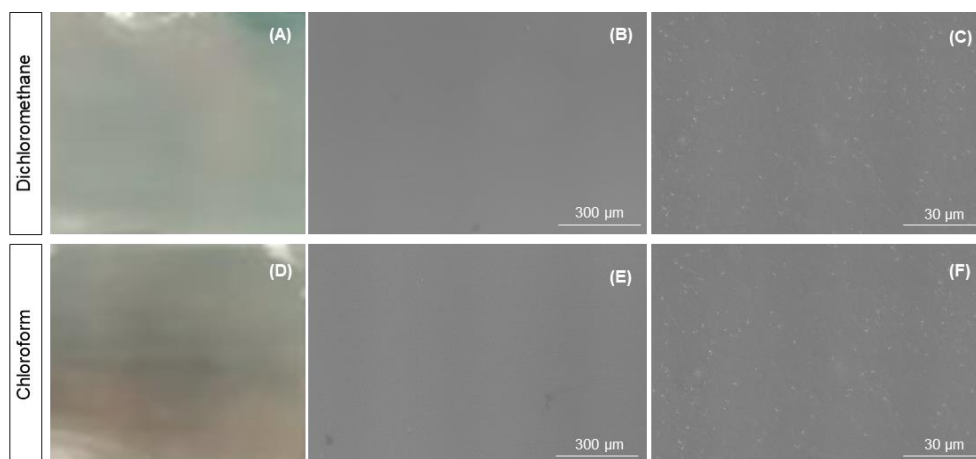


Figure 22 - Photographs of PCL 4% coatings using chloroform (A) and dichloromethane (D) as solvents. Scanning electron microscopy (SEM) micrographs of PCL 4% coatings using chloroform (B,C) and dichloromethane (E, F) as solvents.

At this point, it was possible to obtain two PCL coatings with different solvents that represented two alternatives for the functionalization with compounds P or Q. Each solvent was tested (chloroform or dichloromethane) with P or Q using concentrations of x10 MIC values (156.3 $\mu\text{g/mL}$ and 312.5 $\mu\text{g/mL}$, respectively), hereinafter referred as P10 and Q10. For the functionalization, each compound was previously dissolved in DMSO and added to a solution of 4% (w/v) of PCL. DMSO is an organosulfur compound used as a polar aprotic solvent that by dissolving both polar and nonpolar compounds favor their dissolution in a wide range of organic and aqueous solutions. [73] Once the coatings were synthesized, *Candida albicans* SC5314 cells were cultured on bare and coated plates to assess the efficacy of the compounds in protecting colonization of the surface. For that, the viability of planktonic cells in the supernatant was evaluated as well as the ability to colonize the surface based on the number of viable cells that could be counted upon “scratching” of the plates. The results obtained are shown in Figure 23. In Table v are gathered the CFUs/mL values normalized as ratios between the values obtained in each coated plate and the value for the corresponding bare plate. All the methodology followed in this research is outlined in Annexes – Table vi.

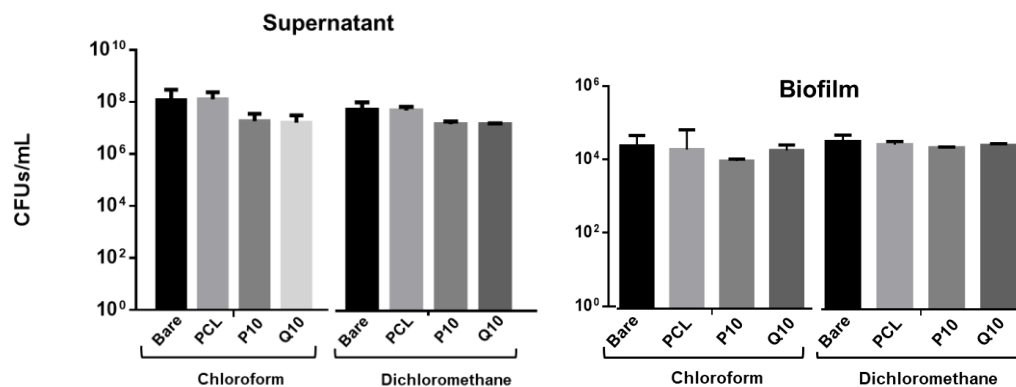


Figure 23 - Graphical representation of CFUs/mL values obtained for each plate in the supernatant and biofilm in the assays using chloroform and dichloromethane as solvent. The results shown are means of, at least, three independent experiments. Bars represent average error. Plates tested were: bare plate, PCL coated plate, PCL plate and compound P at concentrations of x10 MIC values ($\mu\text{g/mL}$) (P10) and PCL plate and compound Q at concentrations of x10 MIC values ($\mu\text{g/mL}$) (Q10).

As represented in Figure 23, PCL coating using chloroform or dichloromethane did not significantly affect the growth of *C. albicans* cells in the supernatant nor the ability of cells to adhere to the surface, since viable cells were collected upon washing and scratching of the surface in both bare or PCL coated plates. This result was also demonstrated by the ratio values obtained (Table v). Remarkably, coating of the surface with P and Q and using both solvents led to a reduction on the ability of *C. albicans* cells to colonize the surface of the material, this being more evident for the P compound (Figure 23) solubilized with chloroform once this solvent resulted in the smallest ratios (Table v).

Table v - Ratios between the CFUs/ mL values obtained in each assay and the values for the bare plates, in both supernatant and biofilm. PCL solvents were chloroform and dichloromethane and the various variants tested were: bare plate, PCL coated plate, PCL plate and compound P at concentrations of x10 and x100 MIC values ($\mu\text{g} / \text{mL}$) (P10 and P100 respectively) and PCL plate and compound Q at concentrations of x10 and x100 MIC values($\mu\text{g} / \text{mL}$) (Q10 and Q100 respectively).

		Bare	PCL	P10	P100	Q10	Q100
Chloroform	Supernatant	1.00	1.06	0.16	0.43	0.13	0.42
	Biofilm	1.00	0.79	0.38	0.86	0.75	0.91
Dichloromethane	Supernatant	1.00	0.90	0.30	-	0.30	-
	Biofilm	1.00	0.83	0.68	-	0.79	-

Chloroform or dichloromethane together with the DMSO used to solubilize the compounds P and Q, were suspected to promote a spatial rearrangement of the PCL and/or compound molecules favoring a prominent antifungal activity, with consequent reduction in cell growth and biofilm formation in the surface of the material. Based on this, the best experimental conditions obtained for functionalization of P and Q on the biomaterial (which were PCL with a concentration of 4%, chloroform as a solvent and a compound concentration of x10 MIC value) were used to better characterize the interaction between the surface of the biomaterial and the *C. albicans* cells. In specific, the properties

of the surface after functionalization (Figure 24) and after colonization (Figure 25) were studied by scanning electron microscopy.

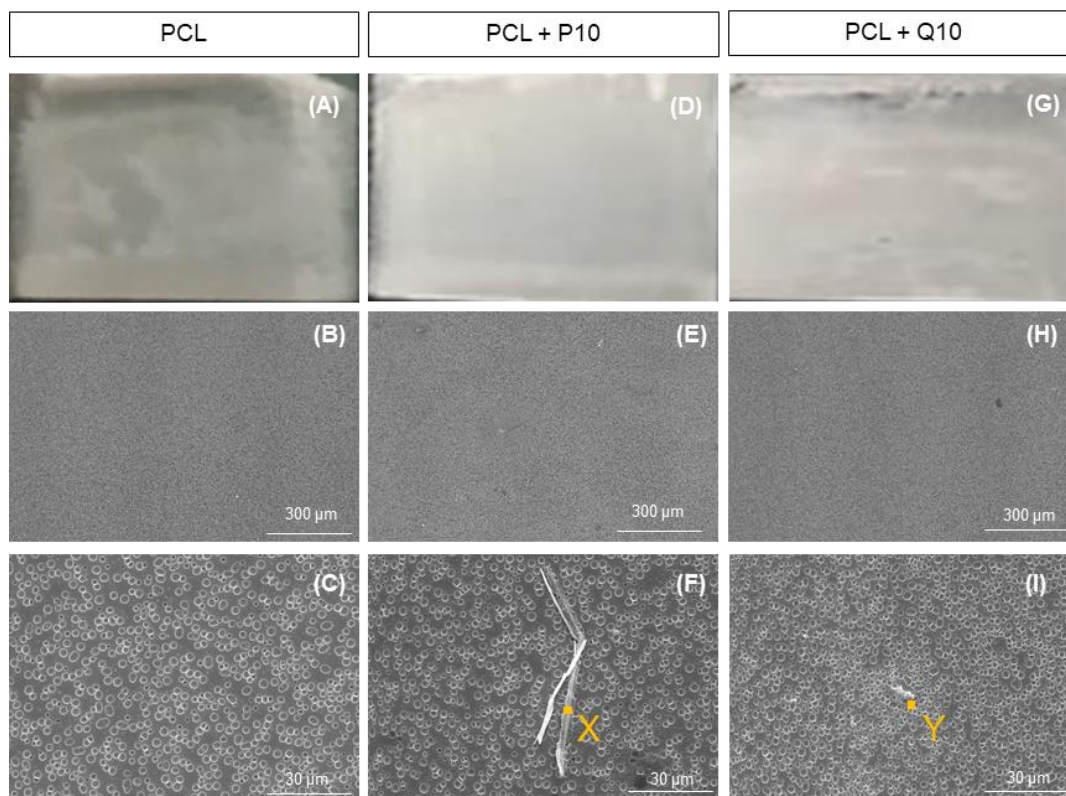


Figure 24 - Photographs of PCL 4% coatings using chloroform as solvent, without compounds (A) and with compound P (D) or Q (G) at concentrations of $\times 10$ MIC values ($\mu\text{g/mL}$). Scanning electron microscopy (SEM) micrographs of PCL 4% coatings using chloroform as solvent, without compounds (B,C) and with compound P (E,F) or Q (H,I) at concentrations of $\times 10$ MIC values ($\mu\text{g/mL}$). Points X and Y mark structures on the coating in which silver was detected.

SEM micrographs showed that DMSO alters the morphology of the PCL coating when compared to the images shown in Figure 22 concerning the result obtained only using chloroform. DMSO presence promotes the appearance of round holes evenly scattered on the surface. Still, these structures did not affect the integrity of the coating, which has remained intact on the plate surface (Figure 24 A). In coatings where compounds P or Q were present, the morphology appears different and it was possible to distinguish different structures on the surfaces, marked by points X and Y, in coatings with P10 and Q10, respectively. According to EDS analysis, were detected 14% of silver at point X and 4% at point Y (Atomic Weight %). These observations suggest that it was in these distinct structures that silver was concentrated on the coatings.

As depicted in Figure 25, cells were able to efficiently adhere to the surface of bare (A) or PCL (B) coated plates, this being consistent with the isolation of a similar number of CFUs upon scratching of the surface of the material (Figure 23). Regarding PCL coating with compounds P or Q (C, D), it was confirmed that the presence of these molecules in the coating made it difficult for *C. albicans* cells to form a biofilm on the surface, as the presence of cells in this surface is significantly lower when

compared to the colonization observed in bare and PCL coated plates. Both compounds appear to have an identical influence in preventing colonization.

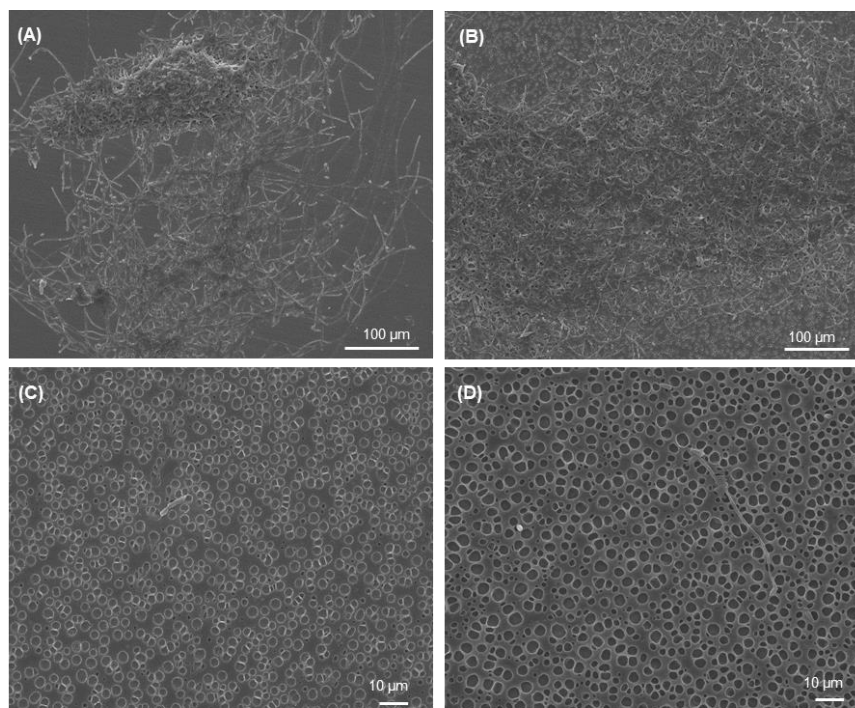


Figure 25 - Colonization of bare and coated steel surfaces by *C. albicans* SC5314 incubated under simulated physiological conditions and corresponding micrographs from SEM: Bare plate (A); PCL coated plate (B); PCL plate and compound P (C) or compound Q (D) at $\times 10$ MIC values ($\mu\text{g/mL}$).

Considering the promising results obtained regarding the functionalization of P and Q compounds with chloroform it was decided to repeat the assay but using concentrations corresponding to 100 times the MIC value (1563 $\mu\text{g/mL}$ for compound P and 3125 $\mu\text{g/mL}$ for compound Q). The results obtained by SEM concerning the properties of the material and colonization by *C. albicans* are shown in Figure 26. Contrary to the initially thought, an increase in the compounds concentration did not result in a significantly augmented effect in prevention of colonization by *C. albicans*. In fact, the number of cells recovered from the surface of the material was higher in this assay than in the one undertaken using P10 or Q10, resulting in a less efficient coating (Figure 26 C). In this result, although unexpected, the chemical environment of the compounds may have been changed by the increased concentration, which could result in distinct compound-polymer interactions, as for instance, compounds preferential aggregation over the solubilization of the polymer.

Indeed, in the P100 assay it is observed a greater surface colonization and it is possible to distinguish different morphologies in the coating, suggesting that the 100-fold concentration alters the chemical bonds, resulting in regions with different morphologies which can be clearly distinguished on the surface of the coating (Figure 26 A). Similarly, this 100-fold increase in the concentration of compound Q (Figure 26 B) compromises the integrity of the coating and holes are formed revealing the underneath substrate and *C. albicans* are preferentially colonizing this surface. The observations in Figure 26 (A, B) really demonstrate the threat these microorganisms pose and the ease with which they attach, grow and adapt to adverse situations. *C. albicans* cells were able to select the areas where the

plate was exposed and start formation of the biofilm from that position. Nevertheless, an interesting observation was obtained in the Q100 assay. It was possible to find large structures scattered on the surface formed by cells and particles with silver (100%, Atomic Weight %) in its composition, detected by EDS in the point X of Fig. 27 D. The appearance of these particles was different from the morphology of compound Q, shown in Figure 19 (C). These *C. albicans* cells are suspected of having the ability to break down the chemical bonds in compound Q, which by being no longer soluble in the coating polymer was exposed to the cells when it is in high concentration. This cleavage facilitates the passage of silver to the zero-oxidation-state and eventually precipitates into nanoparticles. This phenomenon has been described before, in the work of Cardoso (2017) et al. [52], where this strain of *Candida* demonstrates the ability to form silver nanoparticles on the cell's surface.

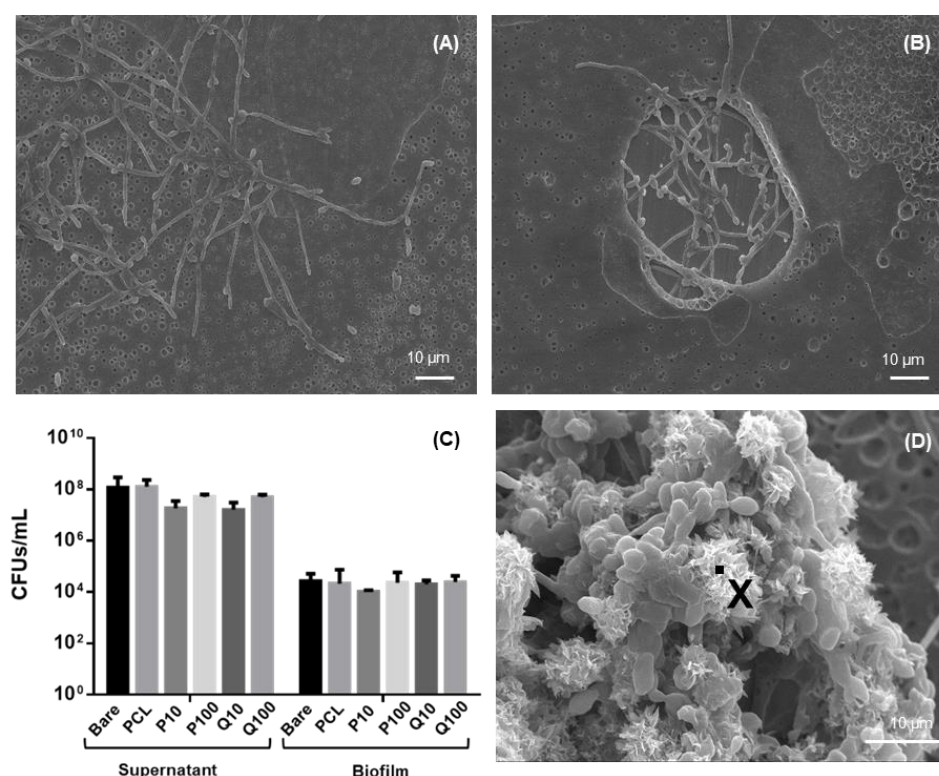


Figure 26 - Colonization of bare and coated steel surfaces by *Candida albicans* SC5314 incubated under simulated physiological conditions and corresponding micrographs from SEM: PCL coated plate and compound P (A) or compound Q (B, D) at x100 MIC values ($\mu\text{g/mL}$). (C): graphical representation of colony forming units per milliliter (CFUs/mL) values obtained for supernatant and biofilm using chloroform as solvent. The number of CFUs in biofilm was quantified after washing and scratching the surface. The number of CFUs present in the supernatant of the cultures that were in contact with the biomaterial was also determined. (D) SEM micrographs of large structures formed by cells and silver particles dispersed on the surface of Q100 coating .

Another objective of this work was achieved, which was the functionalization of medical relevant coatings with the newly synthesized Ag(I)-based camphorimine complexes (Section 3.1.). The assay that yields the most efficient results, that is, which results in lower CFUs/mL values compared to bare plates, was the assay using PCL with a concentration of 4%, chloroform as a solvent and a compound concentration of x10 MIC value.

3.5 Elucidating drug response behaviour *C. albicans* isolates 10A and 22CL

The second part of this thesis is dedicated to a better understanding on the behaviour of the two resistant *C. albicans* isolates, 10A and 22CL, to surpass the deleterious effects of fluconazole. This knowledge is very important in order to better understand what could be the strategies used to counteract the emergence of resistance in *C. albicans*. In Figure 27 it is shown the growth profile of these two isolates in the presence of increasing concentrations of fluconazole, being used the same concentrations that were used to determine the MIC and, consequently, the resistance phenotype of these strains.

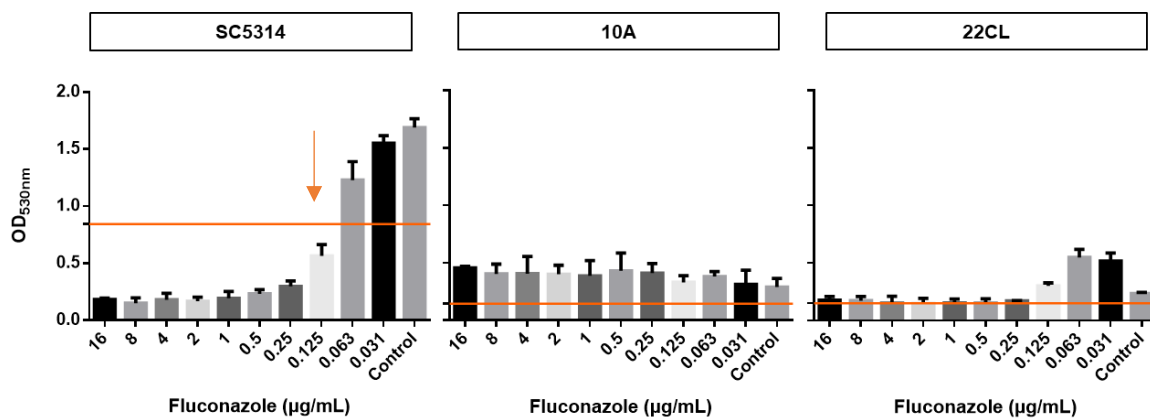


Figure 27 - Microdilution assay for fluconazole against *C. albicans* reference strain SC5314 and strains 10A and 22CL. The MIC value is indicated by an orange arrow and the 50% reduction of the growth registered in the absence of the drug is indicated by the orange line.

The results obtained demonstrated what is considered a normal growth profile of reference strain SC5314 in the presence of fluconazole, where the maximum growth is attained in the absence of the antifungal and progressively decreases as the concentration of drug increases. This pattern was markedly different in strains 10A and 22CL, which exhibited a relatively poor growth (specially when compared with the reference strain SC5314) in control conditions but maintaining that same low level of growth in the remaining concentrations of fluconazole tested. Because of this similarity between the growth profile obtained in control and in the presence of fluconazole, the isolates are classified as resistant. This same unusual phenotype of the 10A and 22CL strains was also obtained when higher concentrations of fluconazole were used as shown in Figure 28.

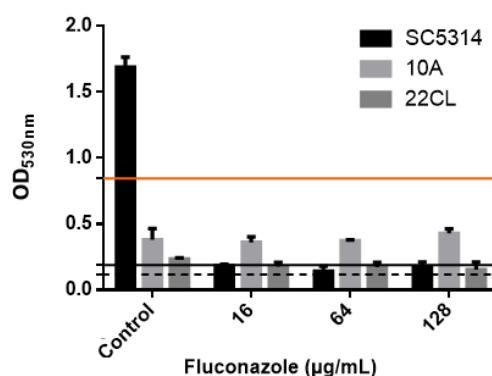


Figure 28 - Microdilution assay for fluconazole in concentrations of 0, 16, 64 and 128 µg/mL, against *C. albicans* reference strain SC5314 and strains 10A and 22CL. The 50% reduction of the growth registered in the absence of drug is indicated by the orange line for strain SC5314, black line for strain 10A and broken line for strain 22CL.

To get further insights into the differences observed among the three strains, the cellular suspensions were observed under the microscope in order to examine whether the differences observed in the OD of the cultures (specially under control conditions) could be attributable to differences in morphology of the cells (Figure 29 A). It was also determined the number of CFUs/mL in the presence or absence of fluconazole (Figure 29 B). It is important to highlight that these procedures were performed under the same experimental conditions that were used to determine the MIC of the strains.

The results obtained showed that under control conditions there was a slight reduction in the number of CFUs obtained from the 22CL and 10A isolates after 24h of cultivation in RPMI in the 96-microwell plates, compared to the number obtained for the SC5314 strain. This was also corroborated by a lower growth rate (growth curve of SC5314, 10A and 22CL strains in Annexes – Figure 36) of the 22CL and 10A strains (0.13 h^{-1} and 0.14 h^{-1} , respectively) compared to the SC5314 strain (0.21 h^{-1}). This difference was, however, much smaller than the one that we observed in the OD of the cultures strongly indicating that there might be something concerning the morphology of the cultures that is affecting the reading of the optical density. Indeed, this is confirmed by microscopy images that show the formation of a robust biofilm formed by the SC5314 cells, while only very small aggregates are observed for the 10A and 22CL isolates (Figure 29 A). In the presence of fluconazole the viability of the 10A cells were always above the one exhibited by the SC5314 strain, while in the case of the 22CL strain this was not observed (Figure 29 B).

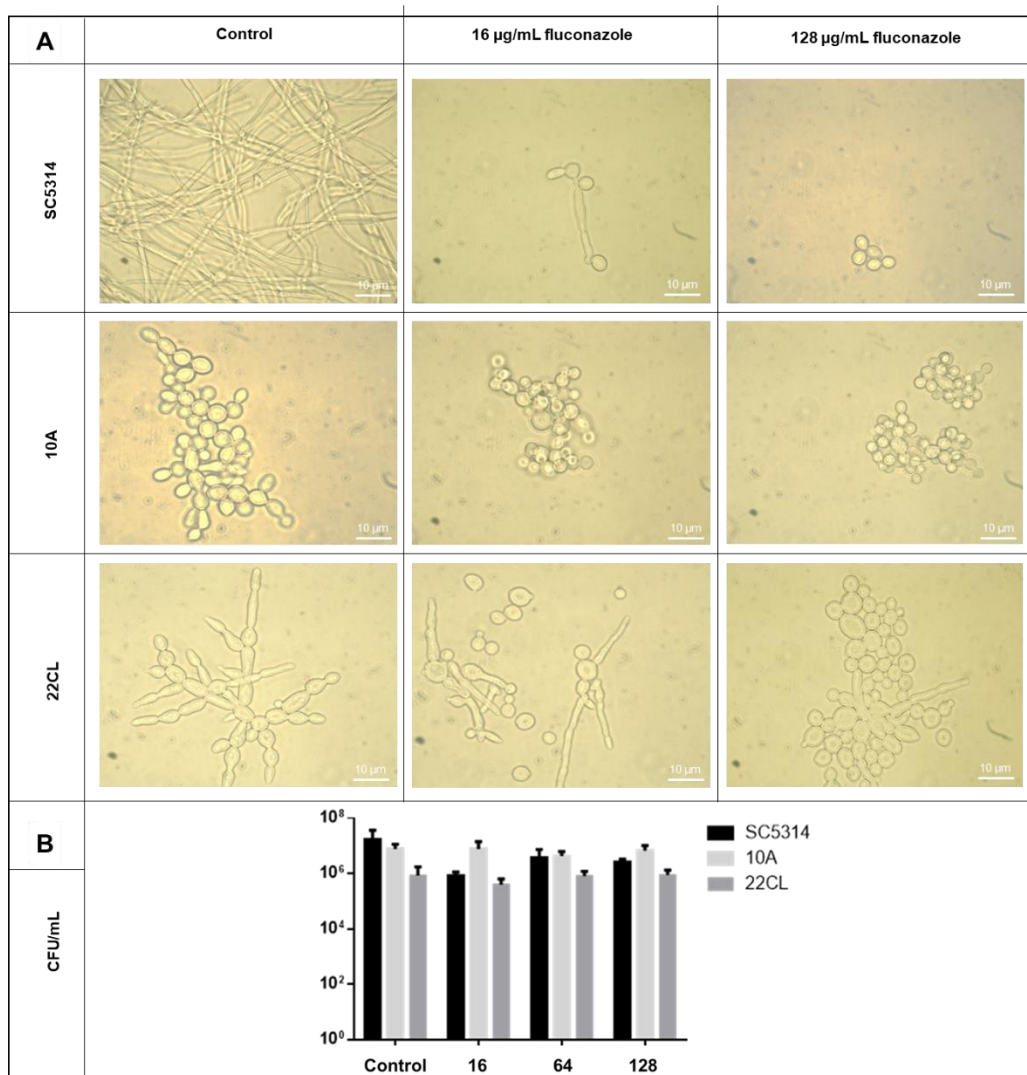


Figure 29 – Observation of cells of strains SC5314, 10A and 22CL under the light microscope after the microdilution assay. Cells exposed to 0 (control), 16 and 128 µg/ml fluconazole were observed (A). Graphical representation of CFUs/mL values obtained for strains SC5314, 10A and 22CL after the microdilution assay with fluconazole concentrations of 0, 16, 64 and 128 µg/mL. The results shown are means of, at least, three independent experiments. Bars represent average errors. (B)

Altogether these results put in question the “resistance phenotype” that is attributed to the 10A and 22CL isolates based on the MIC determination, something that is also corroborated by the observation that the growth curve of these 3 strains in liquid growth medium is identical (Annexes – Figure 36). Although the EUCAST protocol states that the results are valid only if there is growth in the positive control^[9,74] there are no specific guidelines on how to proceed with strain with less conventional growth profiles.

Recently, the observation of “slow”-growing populations within *C. albicans* isolates has been described, these populations being found to contribute for increased resistance and, in some cases, also for increased virulence.^[11] This “slow-growing” population has been found to result from a great phenotypic (and most likely genetic) diversity among clinical strains. Rosenberg et. al.^[11] have classified

this slow-growing population as the fraction of growing cells (or FoG), these being able to grow in concentrations above the MIC and thereby interfering with the classification of resistance and susceptibility of the strains. This ability appears to result from drug response strategies that allow cells to grow slowly despite the drug's ability to interact with its target and to remain in the cell, differing from resistance mechanisms that affect the drug target or its concentration in the cell. It is not clear whether or not the same phenotypic heterogeneity could also be present in the clinical strains 10A and 22CL, however, to get an idea about this disk diffusion assays were performed in conditions that were used before to identify the FoG population (Figure 30 A). Briefly, in these assays it is assessed the ability of cells to grow in the zone of inhibition usually formed in the nearby area surrounding the disks used in the assays. The results obtained using strains SC5314, 10A and 22CL are shown in Figure 30 B.

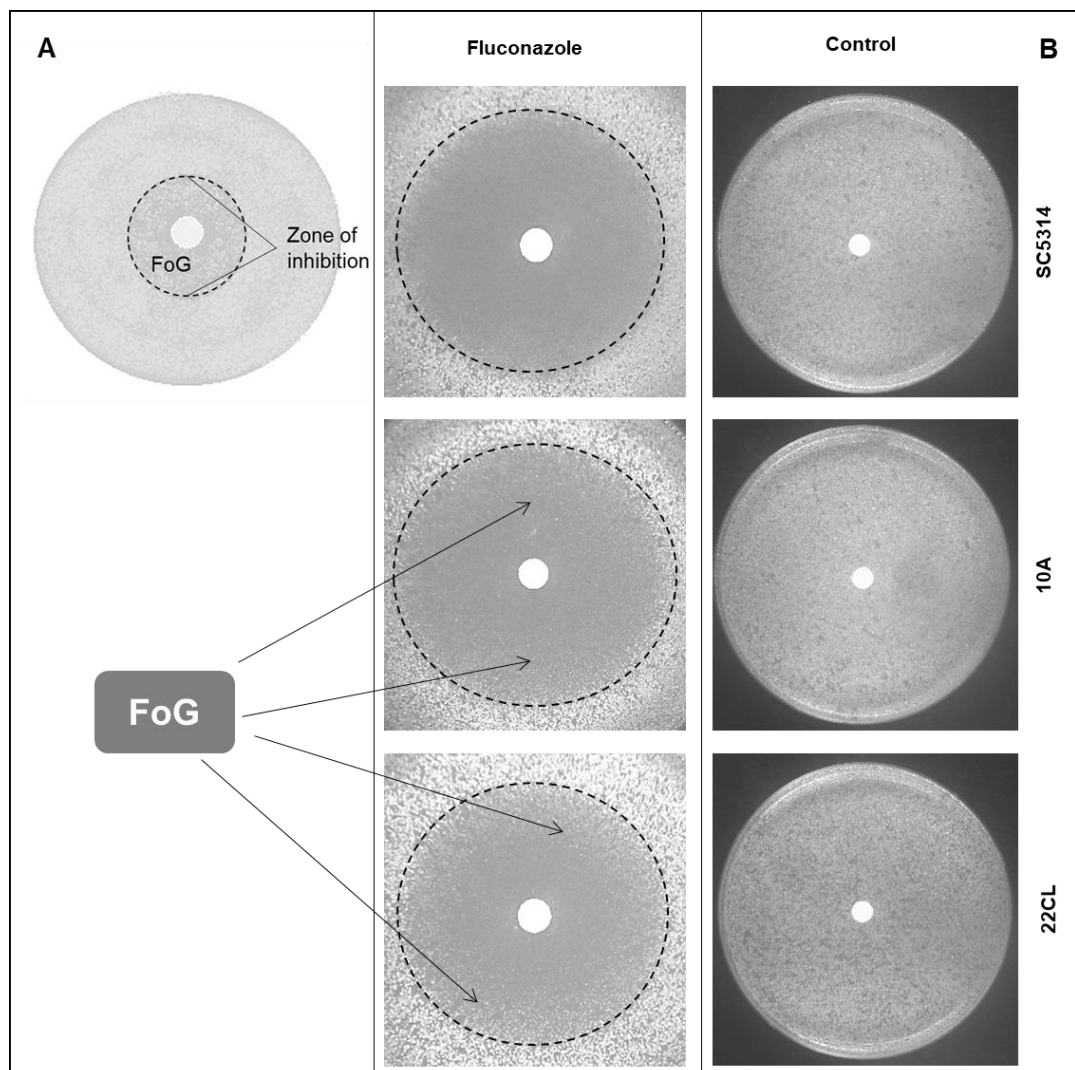


Figure 30 - MHA disk diffusion assay images for strains SC5314, 10A and 22CL in control and in contact with fluconazole. Images on fluconazole discs zoom into the zone of inhibition.

In the disk diffusion assay the aim was to ascertain the existence of colonies growing inside the zone of inhibition. As can be seen from Figure 30 B, there were several colonies that had the ability to grow in the zone of inhibition of fluconazole discs from 10A and 22CL strains, which was not verified for the reference strain. These colonies are named growth fraction (FoG) within the zones of inhibition and medical procedures state that these colonies should be ignored during therapy.^[3] However, Rosenberg et. al.^[11], concluded that these subpopulations are associated with persistent candidemia and also raise the issue that it is necessary to monitor parameters other than MIC, such as FoG, in clinical practice to detect these subpopulations and ensure the most effective therapy. Further studies are needed to ensure that we are dealing with microorganisms with this tolerance capacity and thus clarify their resistance classification.

4 Final Remarks and Future Perspectives

This thesis was aimed at tackling the limitation of existing drugs that address the emerging problem of antifungal resistance in the human pathogens *C. albicans* and *C. glabrata*. This was first achieved by identifying new alternative compounds to the previously used Ag(I)-camphorimine complexes to reach sensitization of *C. albicans* and *C. glabrata*. Then the functionalization of relevant medical coatings with the newly synthesized Ag(I)-based camphorimine complexes P and Q was achieved. The assay that yields the most efficient results was the assay using PCL with a concentration of 4%, chloroform as a solvent and a compound concentration of 156.3 µg/mL of compound P and 312.5 µg/mL of compound Q. The results obtained were very promising and chemical synthesis seems to be a useful tool in the search for new molecules with antimicrobial potential. The large diversity of structures and bonding modes, the great versatility and creativity in the design of novel prospective drugs can be explored in new formulations with antifungal properties. Despite these positive insights, there are still issues to overcome before these compounds can be introduced into clinical practice like the toxicity to mammalian cells, their pharmacokinetic properties and ease of production on a large scale.

Throughout this research, it was possible to establish and optimize experimental conditions that allowed to make coatings with a biodegradable polymer and Ag(I)-derived compounds, with potential to prevent *Candida albicans* surface colonization. Overall, the design of such a complex system required several optimization steps (solvent, polymer concentration, compound concentration, etc), which will then influence other parameters than the anti-*Candida* activity or surface properties, as the effective amount of compound retained in the coating, release profile as well as the coating thickness and adherence to the substrate, all important physicochemical properties that should be assessed in the near future. Furthermore, at this moment, there is no knowledge of the spatial orientation of the molecules in the polymeric matrix. As another future perspective, and in attempt to maximize the optimization the design of these coatings, computational modulation can be used to determine which is the most energy-friendly spatial arrangement in the polymeric matrix used. Another key aspect for this line of research is the study of human cells response to these coatings, as the deleterious effects of the functionalized coating should prevails on fungi and not on human cells. This complex, and yet interesting work is just the tip of the iceberg.

A deeper characterization of the fungi resistance to azoles, can in turn lead to the design of new silver-based compounds, which can then be the base point for the design of new coatings. For that purpose, an attempt was made to further elucidate the mechanisms underlying the resistance to azoles in the resistant *C. albicans* isolates. At this moment, it is essential to bet on the discovery and description of the mechanisms of resistance to antifungals that are increasingly reported but little known. Besides this, it is equally important to ensure that the protocols by which susceptible/resistant classification is sustained address the various behaviors that pathogens can verify in response to the drug, and thus ensure that the classification is unambiguous. This certainty in classification will ensure that the most effective therapy is prescribed and thus provides patients with a better prognosis.

Once these problems are met, it will be easier to develop drugs that have targets other than current drugs, and the design of new chemical compounds can be directed to these new targets. Ideally, with this knowledge we could cope with the growing resistance to antifungals and thus avoid being confined to the limited panoply of existing drugs.

5 References

1. Manolakaki, D., Velmahos, G., Kourkoumpetis, T., Chang, Y., Alam, H., De Moya, M. and Mylonakis, E. *Candida infection and colonization among trauma patients*. *Virulence*, 2010. **1**(5), p.367-375.
2. Silva, S., Negri, M., Henriques, M., Oliveira, R., Williams, D. and Azeredo, J. *Candida glabrata, Candida parapsilosis and Candida tropicalis: biology, epidemiology, pathogenicity and antifungal resistance*. *FEMS Microbiology Reviews*, 2012. **36**(2), p.288-305.
3. Fisher, M., Gow, N. and Gurr, S. *Tackling emerging fungal threats to animal health, food security and ecosystem resilience*. *Philosophical Transactions of the Royal Society B: Biological Sciences*, 2016. **371**(1709), p.20160332.
4. Peron, I., Reichert-Lima, F., Busso-Lopes, A., Nagasako, C., Lyra, L., Moretti, M. and Schreiber, A. *Resistance Surveillance in Candida albicans: A Five-Year Antifungal Susceptibility Evaluation in a Brazilian University Hospital*. *PLOS ONE*, 2016. **11**(7), p.0158126.
5. Ghosh, P., Fisher, M. and Bates, K. *Diagnosing Emerging Fungal Threats: A One Health Perspective*. *Frontiers in Genetics*, 2018. **9**.
6. Perfect, J. (2017). *The antifungal pipeline: a reality check*. *Nature Reviews Drug Discovery*, **16**(9), p.603-616.
7. Brunke, S. and Hube, B. *Two unlike cousins: Candida albicans and C. glabrata infection strategies*. *Cellular Microbiology*, 2013. **15**(5), p.701-708.
8. Gabaldón, T. and Fairhead, C. *Genomes shed light on the secret life of Candida glabrata: not so asexual, not so commensal*. *Current Genetics*, 2018. **65**(1), p.93-98.
9. Arendrup, M., Cuenca-Estrella, M., Lass-Flörl, C. and Hope, W. *EUCAST technical note on the EUCAST definitive document EDef 7.2: method for the determination of broth dilution minimum inhibitory concentrations of antifungal agents for yeasts EDef 7.2 (EUCAST-AFST)**. *Clinical Microbiology and Infection*, 2012. **18**(7), p.E246-E247.
10. Delarze, E. & Sanglard, D. *Defining the frontiers between antifungal resistance, tolerance and the concept of persistence*. *Drug Resist. Updat*, 2015. **23**, 12–19.
11. Rosenberg, A., Ene, I., Bibi, M., Zakin, S., Segal, E., Ziv, N., Dahan, A., Colombo, A., Bennett, R. and Berman, J. *Antifungal tolerance is a subpopulation effect distinct from resistance and is associated with persistent candidemia*. *Nature Communications*, 2018. **9**(1).

12. van Paassen, J., Russcher, A., in 't Veld - van Wingerden, A., Verweij, P. and Kuijper, E. *Emerging aspergillosis by azole-resistant Aspergillus fumigatus at an intensive care unit in the Netherlands, 2010 to 2013*. 2016. *Eurosurveillance*, **21**(30).
13. Salazar, S., Simões, R., Pedro, N., Carvalho, F. and Mira, N. *An Overview On The Fight Against Candidiasis Using Conventional And Non-Conventional Therapeutic Approaches*. *Frontiers in Clinical Drug Research-Anti-Infectives*. 2018 (in press)
14. Silver PM, Oliver BG, White TC. *Role of Candida albicans transcription factor Upc2p in drug resistance and sterol metabolism*. 2004. *Eukaryotic cell*.3(6):1391-7.
15. Sanglard D, Ischer F, Bille J. *Role of ATP-binding-cassette transporter genes in high-frequency acquisition of resistance to azole antifungals in Candida glabrata*. 2001. *Antimicrobial agents and chemotherapy*.45(4):1174-83.
16. Miyazaki H, Miyazaki Y, Geber A, Parkinson T, Hitchcock C, Falconer DJ, et al. *Fluconazole resistance associated with drug efflux and increased transcription of a drug transporter gene, PDH1, in Candida glabrata*. 1998. *Antimicrobial agents and chemotherapy*.42(7):1695-701.
17. Vandeputte P, Larcher G, Berges T, Renier G, Chabasse D, Bouchara JP. *Mechanisms of azole resistance in a clinical isolate of Candida tropicalis*. 2005. *Antimicrobial agents and chemotherapy*.49(11):4608-15.
18. Heilmann CJ, Schneider S, Barker KS, Rogers PD, Morschhauser J. *An A643T mutation in the transcription factor Upc2p causes constitutive ERG11 upregulation and increased fluconazole resistance in Candida albicans*. 2010. *Antimicrobial agents and chemotherapy*.54(1):353-9
19. Alarco AM, Raymond M. *The bZip transcription factor Cap1p is involved in multidrug resistance and oxidative stress response in Candida albicans*. 1999. *Journal of bacteriology*.181(3):700-8.
20. Perlin, D., Rautemaa-Richardson, R. and Alastruey-Izquierdo, A. *The global problem of antifungal resistance: prevalence, mechanisms, and management*. *The Lancet Infectious Diseases*, 2017. **17**(12), p.e383-e392.
21. Fisher, M., Hawkins, N., Sanglard, D. and Gurr, S. *Worldwide emergence of resistance to antifungal drugs challenges human health and food security*. 2018. *Science*,. **360**(6390), p.739-742.
22. Lepak, A., Zhao, M., VanScoy, B., Ambrose, P. and Andes, D. *Pharmacodynamics of a Long-Acting Echinocandin, CD101, in a Neutropenic Invasive-Candidiasis Murine Model Using an Extended-Interval Dosing Design*. 2017. *Antimicrobial Agents and Chemotherapy*, **62**(2), p.66-70.
23. Campoy, S. and Adrio, J. *Antifungals*. 2017. *Biochemical Pharmacology*, **133**, pp.86-96.

24. Arendrup, M., Jensen, R. and Cuenca-Estrella, M. *In Vitro Activity of ASP2397 against Aspergillus Isolates with or without Acquired Azole Resistance Mechanisms*. *Antimicrobial Agents and Chemotherapy*, 2015. **60**(1), p.532-536.
25. Alves, C., Ferreira, I., Barros, L., Silva, S., Azeredo, J. and Henriques, M. *Antifungal activity of phenolic compounds identified in flowers from North Eastern Portugal against Candida species*. *Future Microbiology*, 2014. **9**(2), p.139-146.
26. Krzyściak, W., Kościelniak, D., Papież, M., Vyhouskaya, P., Zagórska-Świeży, K., Kołodziej, I., Bystrowska, B. and Jurczak, A. *Effect of a Lactobacillus Salivarius Probiotic on a Double-Species Streptococcus Mutans and Candida Albicans Caries Biofilm*. *Nutrients*, 2017. **9**(11), p.1242.
27. Kovachev, S. and Vatcheva-Dobrevska, R. *Local Probiotic Therapy for Vaginal Candida albicans Infections*. *Probiotics and Antimicrobial Proteins*, 2014. **7**(1), p.38-44.
28. Zhao, C., Lv, X., Fu, J., He, C., Hua, H. and Yan, Z. *In vitro inhibitory activity of probiotic products against oral Candida species*. *Journal of Applied Microbiology*, 2016. **121**(1), p.254-262.
29. Criseo, G., Scordino, F. and Romeo, O. *Current methods for identifying clinically important cryptic Candida species*. *Journal of Microbiological Methods*, 2015. **111**, p.50-56.
30. Yapar, N. *Epidemiology and risk factors for invasive candidiasis*. *Therapeutics and Clinical Risk Management*, 2014. p.95.
31. Moazeni, M., Khoramizadeh, M., Teimoori-Toolabi, L., Noorbakhsh, F. Fallahi AA., Rezaie, S. *Down-regulation of the ALS3 gene as a consequent effect of RNA-mediated silencing of the EFG1 gene in Candida albicans*. *Iran Biomed J.* 2012. **16**(4):172-8.
32. Nishikawa, J., Boeszoermenyi, A., Vale-Silva, L., Torelli, R., Posteraro, B., Sohn, Y., Ji, F., Gelev, V., Sanglard, D., Sanguinetti, M., Sadreyev, R., Mukherjee, G., Bhyravabhotla, J., Buhrlage, S., Gray, N., Wagner, G., Näär, A. and Arthanari, H. *Inhibiting fungal multidrug resistance by disrupting an activator–Mediator interaction*. *Nature*, 2016. **530**(7591), pp.485-489.
33. Yin C, Wong JH, Ng TB. *Recent studies on the antimicrobial peptides lactoferricin and lactoferrampin*. *Curr. Mol. Med.* 2014. **14**(9), 1139–1154.
34. Polonelli, L., Ciociola, T., Elviri, L., Zanello, P., Giovati, L., Arruda, D., Muñoz, J., Mortara, R., Morace, G., Borghi, E., Galati, S., Marin, O., Casoli, C., Pilotti, E., Ronzi, P., Travassos, L., Magliani, W. and Conti, S. *A Naturally Occurring Antibody Fragment Neutralizes Infectivity of Diverse Infectious Agents*. *Scientific Reports*, 2016. **6**(1).
35. Rossi, D., Munoz, J., Carvalho, D., Belmonte, R., Faintuch, B., Borelli, P., Miranda, A., Taborda, C. and Daffre, S. *Therapeutic use of a cationic antimicrobial peptide from the*

- spider Acanthoscurria gomesiana in the control of experimental candidiasis*. BMC Microbiology, 2012. **12**(1), p.28.
36. Wang K, Dang W, Xie J et al. *Antimicrobial peptide protonectin disturbs the membrane integrity and induces ROS production in yeast cells*. BBA Biomembranes, 2015. **1848**(10, Part A), 2365–2373.
 37. andal SM, Migliolo L, Franco OL, Ghosh AK. *Identification of an antifungal peptide from Trapa natans fruits with inhibitory effects on Candida tropicalis biofilm formation*. Peptides 2011. **32**(8), 1741–1747.
 38. Delattin N, De Brucker K, Craik DJ et al. *Plant-derived decapeptide OSIP108 interferes with Candida albicans biofilm formation without affecting cell viability*. Antimicrob. Agents Chemother. 2014. **58**(5), 2647–2656.
 39. Sun, Q., Li, J. and Le, T. Zinc Oxide Nanoparticle as a Novel Class of Antifungal Agents: Current Advances and Future Perspectives. Journal of Agricultural and Food Chemistry, 2018. **66**(43), pp.11209-11220.
 40. Edwards, J., Schwartz, M., Schmidt, C., Sobel, J., Nyirjesy, P., Schodel, F., Marchus, E., Lizakowski, M., DeMontigny, E., et al. *A Fungal Immunotherapeutic Vaccine (NDV-3A) for Treatment of Recurrent Vulvovaginal Candidiasis—A Phase 2 Randomized, Double-Blind, Placebo-Controlled Trial*. Clinical Infectious Diseases, 2018. **66**(12), p.1928-1936.
 41. Pianalto, K. and Alspaugh, J. *New Horizons in Antifungal Therapy*. Journal of Fungi, 2016. **2**(4), p.26.
 42. Apgar, J., Wilkening, R., Greenlee, M., Balkovec, J., Flattery, A., Abruzzo, G., Galgoci, A., Giacobbe, R., Gill, C., Hsu, M., Liberator, P., Misura, A., Motyl, M., Nielsen Kahn, J., Powles, M., Racine, F., Dragovic, J., Habulihaz, B., Fan, W., Kirwan, R., Lee, S., Liu, H., Mamai, A., Nelson, K. and Peel, M. *Novel orally active inhibitors of β -1,3-glucan synthesis derived from enfumafungin*. Bioorganic & Medicinal Chemistry Letters, 2015. **25**(24), pp.5813-5818.
 43. G. Wang, X. Li and Z. Wang *APD3: the antimicrobial peptide database as a tool for research and education*, Nucleic Acids Research, 2016. Vol. **44**, Database issue: D1087-D1093.
 44. Souza, M., Lopes, L., Bonez, P., Gündel, A., Martinez, D., Sagrillo, M., Giongo, J., Vaucher, R., Raffin, R., Boligon, A. and Santos, R. *Melaleuca alternifolia nanoparticles against Candida species biofilms*. 2017. Microbial Pathogenesis, 104, pp.125-132.
 45. Sholkamy, E., Ahamd, M., Yasser, M. and Eslam, N. *Anti-microbiological activities of bio-synthesized silver Nano-stars by Saccharopolyspora hirsuta*. 2019. Saudi Journal of Biological Sciences, 26(1), pp.195-200.

46. Durán, N., Nakazato, G. and Seabra, A. *Antimicrobial activity of biogenic silver nanoparticles, and silver chloride nanoparticles: an overview and comments*. Applied Microbiology and Biotechnology, 2016. 100(15), pp.6555-6570.
47. Savić, N., Vojnovic, S., Glišić, B., Crochet, A., Pavic, A., Janjić, G., Pekmezović, M., Opsenica, I., Fromm, K., Nikodinovic-Runic, J. and Djuran, M. Mononuclear silver(I) complexes with 1,7-phenanthroline as potent inhibitors of *Candida* growth. European Journal of Medicinal Chemistry, 2018. **156**, pp.760-773.
48. Monteiro, D., Gorup, L., Silva, S., Negri, M., de Camargo, E., Oliveira, R., Barbosa, D. and Henriques, M. *Silver colloidal nanoparticles: antifungal effect against adhered cells and biofilms of Candida albicans and Candida glabrata*. Biofouling, 2011. **27**(7), pp.711-719.
49. Shao, P., Huang, L. and Hsueh, P. *Recent advances and challenges in the treatment of invasive fungal infections*. 2007. International Journal of Antimicrobial Agents, 30(6), pp.487-495.
50. Matsumura Y, Yoshikata K, Kunisaki S, Tsuchido T. *Mode of bacterial action of silver zeolite and its comparison with that of silver nitrate*. Appl. Environ. Microbiol. 2003. **69**: 4278–4281.
51. Molnár, Z., Bódai, V., Szakacs, G., Erdélyi, B., Fogarassy, Z., Sáfrán, G., Varga, T., Kónya, Z., Tóth-Szeles, E., Szűcs, R. and Lagzi, I. *Green synthesis of gold nanoparticles by thermophilic filamentous fungi*. 2018. Scientific Reports, 8(1).
52. Cardoso JMS, Guerreiro SI, Lourenço A, Alves MM, Montemor MF, Mira NP, Leitão JH, Carvalho MFNN. *Ag(I) camphorimine complexes with antimicrobial activity towards clinically important bacteria and species of the Candida genus*. PLoS ONE, 2017. **12**(5): e0177355
53. Casini, A., Bonsignore, R. and Oberkofler, J. *Organometallic Gold-Based Anticancer Therapeutics*. Reference Module in Chemistry, Molecular Sciences and Chemical Engineering. 2018.
54. Pappas, P. G., Lionakis, M. S., Arendrup, M. C., Ostrosky-Zeichner, L., & Kullberg, B. J. *Invasive candidiasis*. 2018. Nature Reviews Disease Primers, **4**, 18026.
55. Kotha, S. and Meshram, M. *Application of organometallics in organic synthesis*. Journal of Organometallic Chemistry, 2018. **874**, pp.13-25.
56. Malachová, K., Praus, P., Rybková, Z. and Kozák, O. *Antibacterial and antifungal activities of silver, copper and zinc montmorillonites*. Applied Clay Science, 2011. **53**(4), pp.642-645.
57. Grass, G., Rensing, C. and Solioz, M. *Metallic Copper as an Antimicrobial Surface*. Applied and Environmental Microbiology, 2010. **77**(5), pp.1541-1547.

58. Roe, D., Karandikar, B., Bonn-Savage, N., Gibbins, B. and Roulet, J. *Antimicrobial surface functionalization of plastic catheters by silver nanoparticles*. Journal of Antimicrobial Chemotherapy, 2008. **61**(4), pp.869-876..
59. Roe, D., Karandikar, B., Bonn-Savage, N., Gibbins, B. and Roulet, J. *Antimicrobial surface functionalization of plastic catheters by silver nanoparticles*. Journal of Antimicrobial Chemotherapy, 2008. **61**(4), pp.869-876.
60. M. Quinn, F. Milder, The Science of Oligon (<http://ht.edwards.com/resourcegallery/products/centralvenousaccess/pdfs/scienceofoligon112.pdf>. Accessed on: January 29, 2019) Lifesciences, Irvine, CA, 2002.
61. Szweda, P., Gorczyca, G. and Tylingo, R. *Comparison of antimicrobial activity of selected, commercially available wound dressing materials*. 2018 Journal of Wound Care, 27(5), pp.320-326.
62. Wounds-uk.com. (2019). [online] Available at: <https://www.wounds-uk.com/download/resource/5963> [Accessed 30 Jan. 2019].
63. Marques, L., Alves, M., Eugénio, S., Salazar, S., Pedro, N., Grenho, L., Mira, N., Fernandes, M. and Montemor, M. Potential anti-cancer and anti-Candida activity of Zn-derived foams. Journal of Materials Chemistry B, 2018. **6**(18), pp.2821-2830.
64. Alves, M., Cunha, D., Santos, C., Mira, N. and Montemor, M. Microstructured ZnO-rod like coating prevents biofilm formation prompted by pathogenic Candida spp. Ceramics International, 2018. **44**(4), pp.4467-4472.
65. Mohandas, A., Deepthi, S., Biswas, R., & Jayakumar, R. *Chitosan based metallic nanocomposite scaffolds as antimicrobial wound dressings*. Bioactive Materials, 2018. **3**(3), 267–277.
66. Pippi, B., Machado, G., Bergamo, V., Alves, R., Andrade, S. and Fuentefria, A. *Clioquinol is a promising preventive morphological switching compound in the treatment of Candida infections linked to the use of intrauterine devices*. Journal of Medical Microbiology, 2018. **67**(11), pp.1655-1663.
67. Novais, D. *Studying mechanisms of antifungal resistance in Candida glabrata clinical isolates: emphasis on the role of the CgPdr1 transcription factor*. Master. 2017 Universidade de Lisboa: Faculdade de Ciências.
68. Malachová, K., Praus, P., Rybková, Z. and Kozák, O. *Antibacterial and antifungal activities of silver, copper and zinc montmorillonites*. 2011. Applied Clay Science, 53(4), pp.642-645.
69. Salazar, S., Wang, C., Münsterkötter, M., Okamoto, M., Takahashi-Nakaguchi, A., Chibana, H., Lopes, M., Güldener, U., Butler, G. and Mira, N. *Comparative genomic and transcriptomic analyses unveil novel features of azole resistance and adaptation to the human host in Candida glabrata*. FEMS Yeast Research, 2017. **18**(1).

70. Souza, J., Alves, M., Barbosa, D., Lopes, M., Pinto, E., Figueiral, M., Delbem, A. and Mira, N. *Study of the activity of Punica granatum-mediated silver nanoparticles against Candida albicans and Candida glabrata, alone or in combination with azoles or polyenes*. 2019. Medical Mycology.
71. Yang, K. and Ren, Y. *Nickel-free austenitic stainless steels for medical applications*. Science and Technology of Advanced Materials, 2010. **11**(1), p.014105.
72. Solomon, K., Velders, G., Wilson, S., Madronich, S., Longstreth, J., Aucamp, P. and Bornman, J. *Sources, fates, toxicity, and risks of trifluoroacetic acid and its salts: Relevance to substances regulated under the Montreal and Kyoto Protocols*. Journal of Toxicology and Environmental Health, Part B, 2016. **19**(7), p.289-304.
73. León-García, M., Ríos-Castro, E., López-Romero, E. and Cuéllar-Cruz, M. *Evaluation of cell wall damage by dimethyl sulfoxide in Candida species*. Research in Microbiology, 2017. **168**(8), p.732-739.
74. Eucast.org. (2019). [online] Available at: http://www.eucast.org/fileadmin/src/media/PDFs/EUCAST_files/Disk_test_documents/2019_manuals/Reading_guide_BMD_v_1.0_2019.pdf [Accessed 30 Aug. 2019].

6 Annexes

Annex A

Spectroscopic details for the camphor ligands and copper and zinc complexes

C₃₂H₃₆N₂O₂ (L1)

FTIR (cm⁻¹): 1746 (ν_{CO}), 1661 (ν_{CN}).

¹H NMR (CDCl₃, 400 MHz): δ 7.61 (d, *J*=8.3 Hz, 4H), 7.02 (d, *J*=8.3 Hz, 4H), 2.91 (d, *J*=4.6 Hz, 2H), 1.13 (s, 6H), 1.01 (s, 6H), 0.94 (s, 6H) ppm.

¹³C NMR (CDCl₃, 400 MHz) δ 206.5, 172.0, 148.8, 137.7, 127.5, 121.4, 58.2, 50.4, 44.8, 30.3, 24.6, 21.2, 17.7, 9.2 ppm.

C₂₆H₃₂N₂O₂ (L2)

FTIR (cm⁻¹): 1755 (ν_{CO}), 1684 (ν_{CN}).

¹H NMR (CDCl₃, 400 MHz): δ 6.98 (s, 4H), 2.91 (d, *J*=4.6 Hz, 2H), 1.12 (s, 6H), 1.01 (s, 6H), 0.92 (s, 6H) ppm.

¹³C NMR (CDCl₃, 400 MHz) δ 206.5, 171.8, 146.9, 121.9, 58.2, 50.4, 44.9, 30.3, 24.5, 21.1, 17.7, 9.2 ppm.

C₂₆H₃₂N₂O₂ (L3)

FTIR (cm⁻¹): 1753 (ν_{CO}), 1674 (ν_{CN}).

¹H NMR (CDCl₃, 400 MHz): δ 7.38 (t, 1H), 6.75 (dd, 2H), 6.42 (s, 1H), 2.85 (d, *J*=4.7 Hz, 2H), 1.13 (s, 6H), 1.01 (s, 6H), 0.94 (s, 6H) ppm.

¹³C NMR (CDCl₃, 400 MHz) δ 206.3, 172.5, 150.5, 129.7, 117.0, 111.3, 58.2, 50.1, 44.5, 30.1, 24.4, 21.0, 17.5, 9.0 ppm.

[(CuCl₂)(L1)] (A)

FTIR (cm⁻¹): 1750 (ν_{CO}), 1675 (ν_{CN}).

It is not possible to obtain NMR spectra for this element (Cu(II)) due to its paramagnetic character.

Elem. Anal. (%) for [(CuCl₂)L1]: Found: C, 47.6; N, 8.5; H, 6.7. Calc.: C, 48.0; N, 8.2; H, 6.5.

[(CuCl₂)(L3)] (C)

FTIR (cm⁻¹): 1747 (ν_{CO}), 1633 (ν_{CN}).

It is not possible to obtain NMR spectra for this element (Cu(II)) due to its paramagnetic character.

Elem. Anal. (%) for [(CuCl₂)₃L3].4THF₂: Found: C, 49.2; N, 5.0; H, 5.2. Calc.: C, 49.4; N, 4.8; H, 5.5.

[(Cu(NO₃)₂)(L1)] (F)

FTIR (cm⁻¹): 1748 (ν_{CO}), 1656 (ν_{CN}).

It is not possible to obtain NMR spectra for this element (Cu(II)) due to its paramagnetic character.

Elem. Anal. (%) for [(Cu(NO₃)₂)(L1)]: Found: C, 56.2; N, 7.4; H, 5.8. Calc.: C, 56.0; N, 8.2; H, 5.6.

[(Cu(NO₃)₂)(L3)] (G)

FTIR (cm⁻¹): 1748 (ν_{CO}), 1656 (ν_{CN}).

It is not possible to obtain NMR spectra for this element (Cu(II)) due to its paramagnetic character.

Elem. Anal. (%) for [(Cu(NO₃)₂)(L3)]: Found: C, 52.9; N, 8.1; H, 5.8. Calc.: C, 52.7; N, 9.5; H, 5.5.

[(CuCl)₂(L1)] (I)

FTIR (cm⁻¹): 1740 (ν_{CO}), 1624 (ν_{CN}).

¹H NMR (CDCl₃, 400 MHz): δ 7.70 (d, *J*=7.4 Hz, 4H), 7.02 (d, *J*=7.2 Hz, 4H), 2.82 (s, 2H), 1.05 (s, 6H), 0.99 (s, 6H), 0.88 (s, 6H) ppm.

¹³C NMR (CD₃CN, 400 MHz): not obtained due to decomposition during acquisition

Elem. Anal. (%) for [(CuCl₂)(L1)_½·H₂O]: Found: C, 56.1; N, 4.0; H, 5.5. Calc.: C, 56.2; N, 4.1; H, 5.3.

[(CuCl)₂(L2)] (J)

FTIR (cm⁻¹): 1749 (ν_{CO}), 1638 (ν_{CN}).

¹H NMR (CD₃CN, 400 MHz): δ 6.99 (s, 4H), 2.85 (s, 2H), 1.05 (s, 6H), 1.00 (s, 6H), 0.86 (s, 6H) ppm.

¹³C NMR (CD₃CN, 400 MHz): not obtained due to decomposition during acquisition

Elem. Anal. (%) for [(CuCl₂)(L2)_½·H₂O]: Found: C, 49.6; N, 4.1; H, 5.6. Calc.: C, 49.9; N, 4.3; H, 5.3.

[(ZnCl₂)(THF)(L1)] (L)

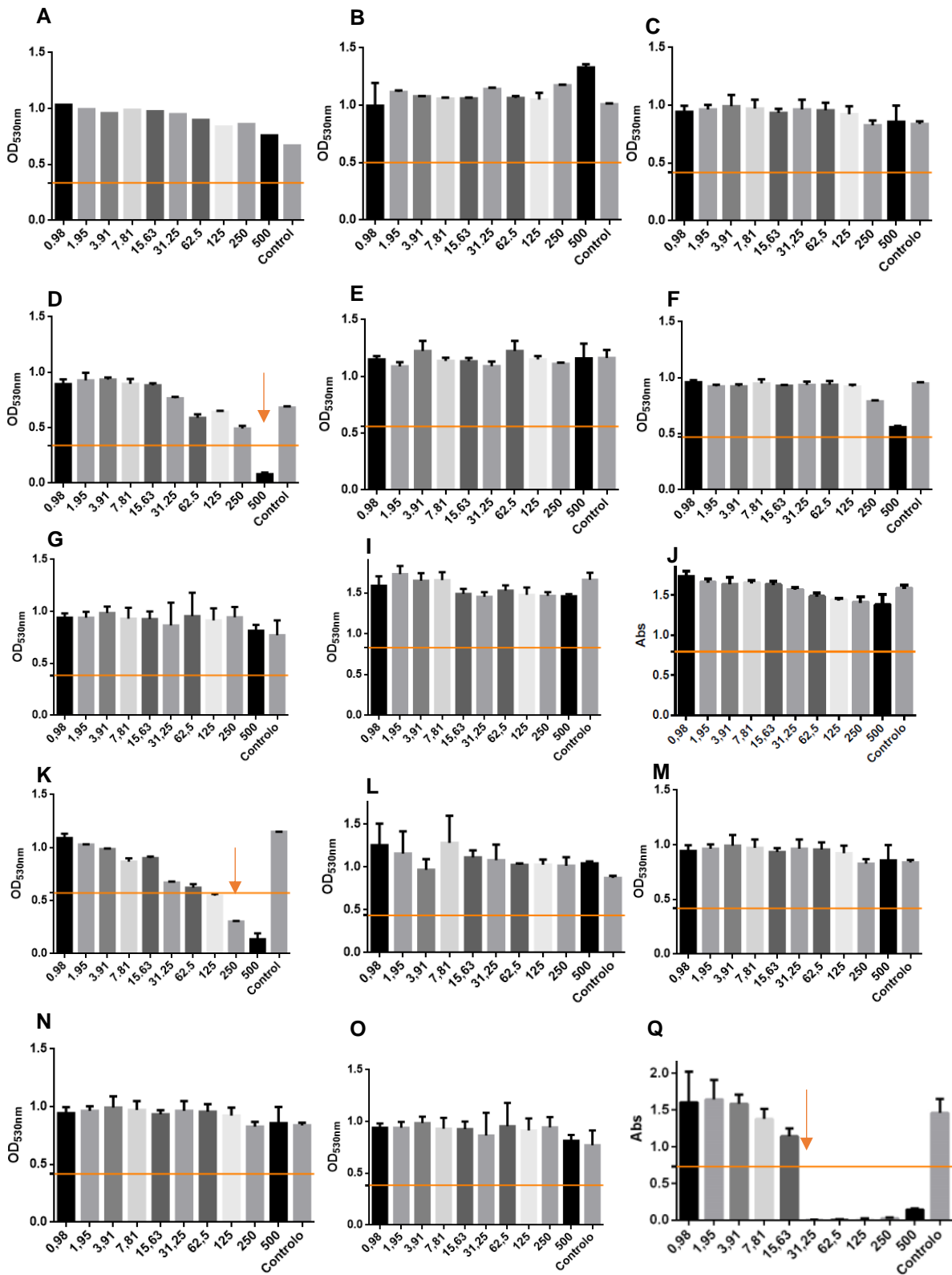
FTIR (cm⁻¹): 1749 (ν_{CO}), 1617 (ν_{CCarom}).

¹H NMR (CD₃CN, 400 MHz): δ 7.72 (d, *J*=7.6 Hz, 4H), 7.08 (d, *J*=7.0 Hz, 4H), 2.88 (d, *J*=3.2 Hz, 2H), 1.08 (s, 6H), 1.01 (s, 6H), 0.88 (s, 6H) ppm.

¹³C NMR (CD₃CN, 400 MHz) δ 207.5, 174.1, 150.5, 128.5, 122.4, 68.3, 58.9, 51.3, 45.6, 30.9, 26.2, 24.8, 21.3, 17.5, 9.3 ppm.

%. Elem. Anal. (%) for [(ZnCl₂)₂L1]·4H₂O: Found: C, 46.4; N, 2.9; H, 5.2. Calc.: C, 46.5; N, 3.4; H, 5.4.

Annex B



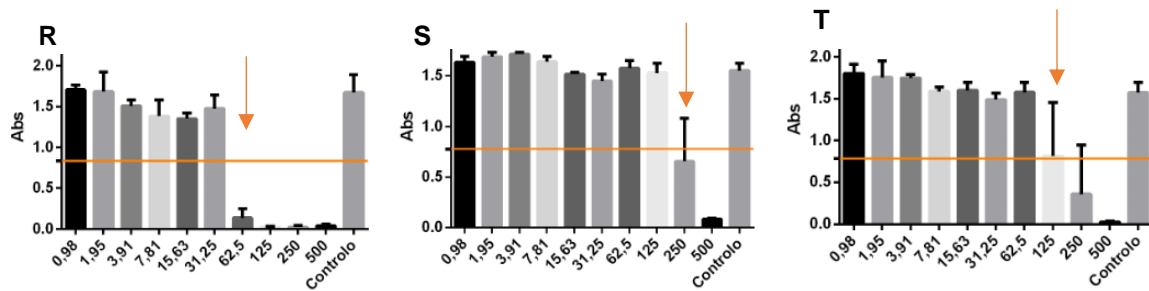
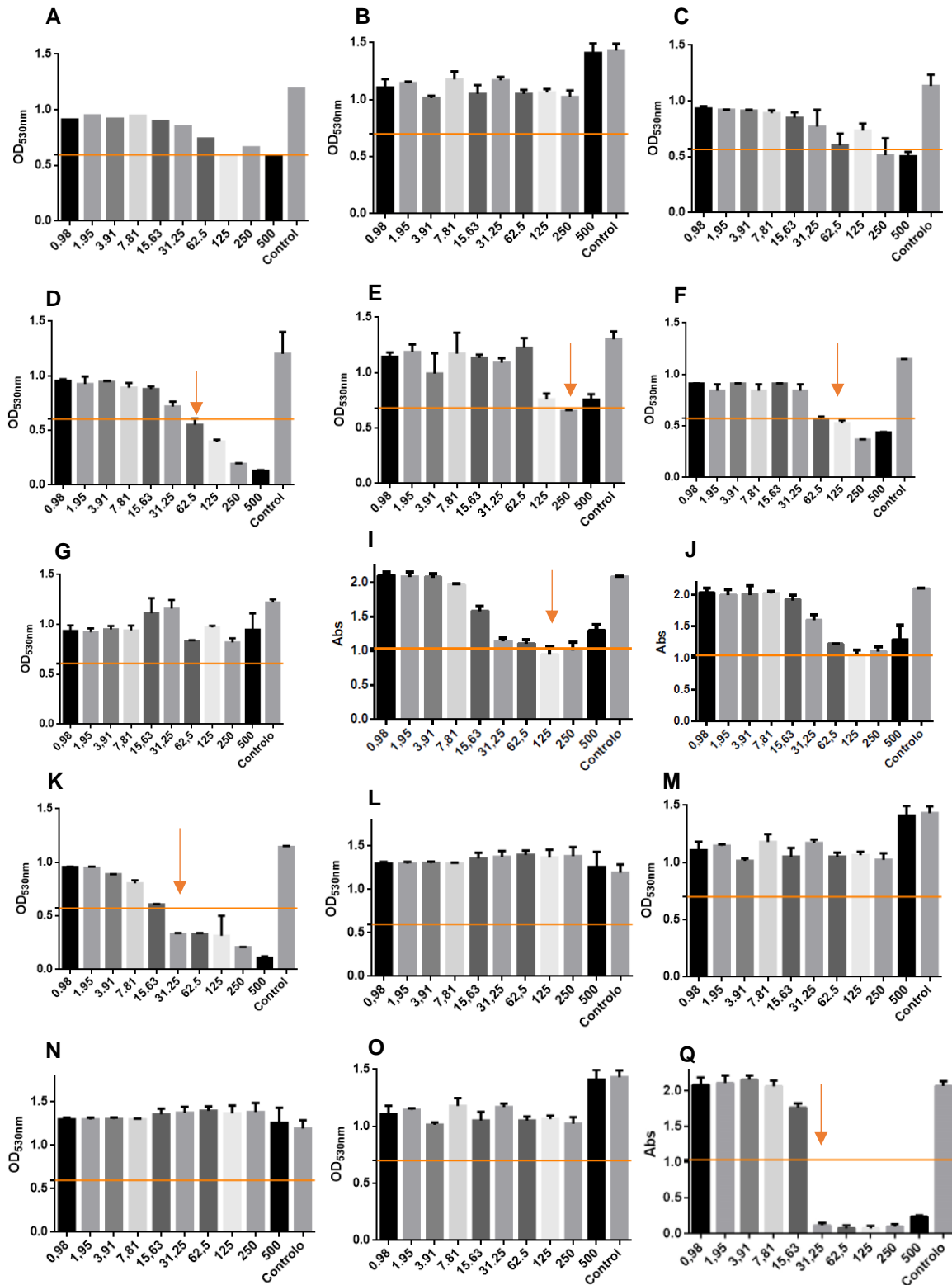


Figure 31 - Microdilution assay for all the complexes (A-T) against the reference species *C. albicans* SC5314. The MIC value is indicated by an orange arrow and the 50% reduction of the growth registered in the absence of the chemicals is indicated by the orange line.

Annex C



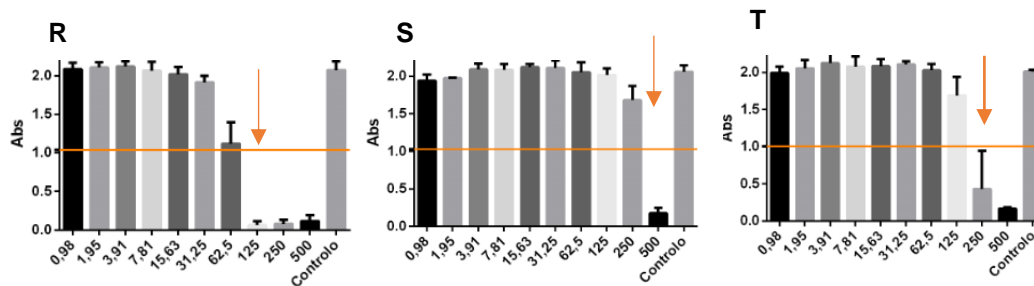


Figure 32 -Microdilution assay for all the complexes (A-T) against the reference species *C. glabrata* CBS138. The MIC value is indicated by an orange arrow and the 50% reduction of the growth registered in the absence of the chemicals is indicated by the orange line

Annex D

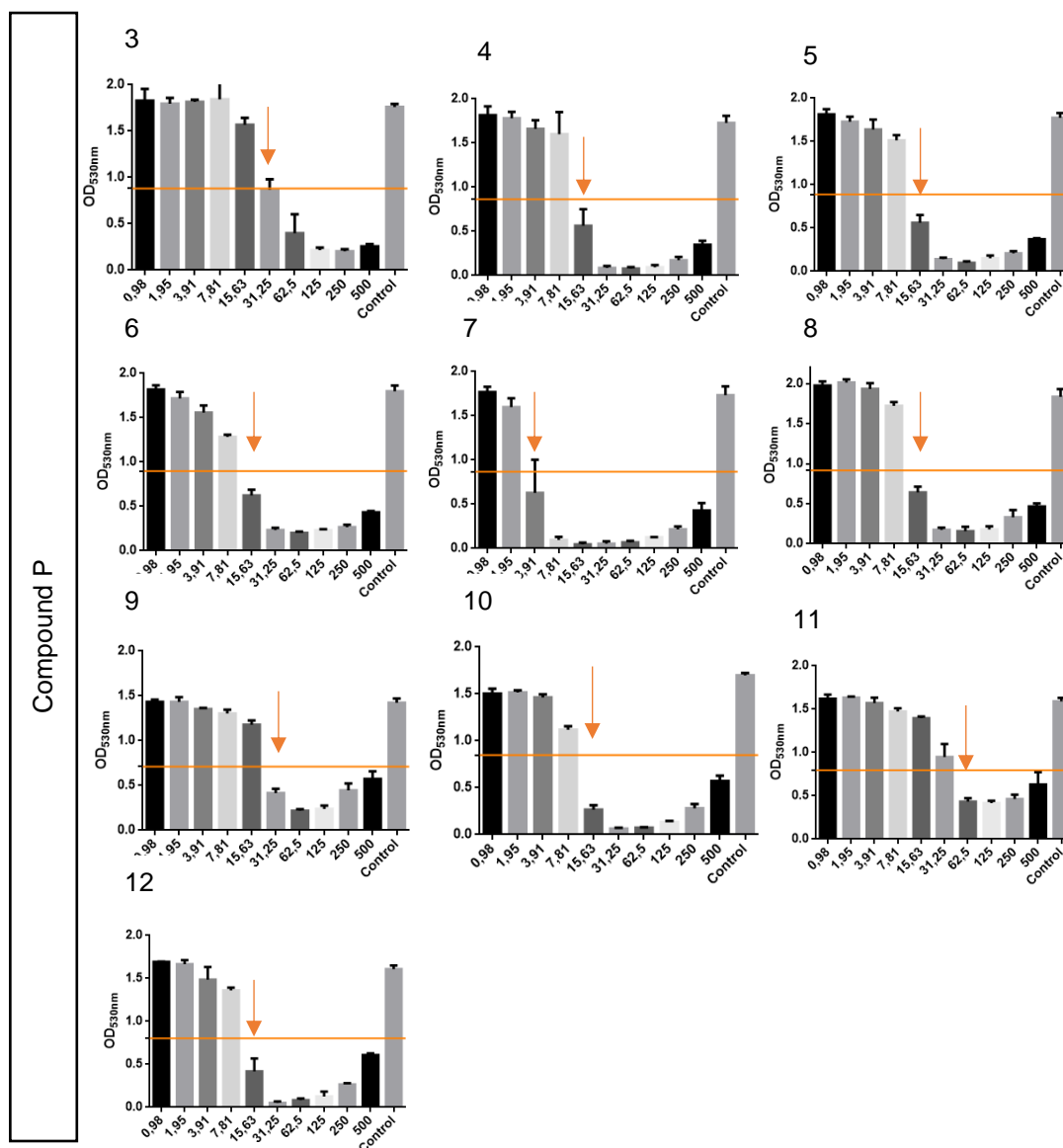


Figure 33 - Microdilution assay for all the complexes P against the azole resistant isolates of *C. glabrata* (3-12). The MIC value is indicated by an orange arrow and the 50% reduction of the growth registered in the absence of the chemicals is indicated by the orange line.

Annex E

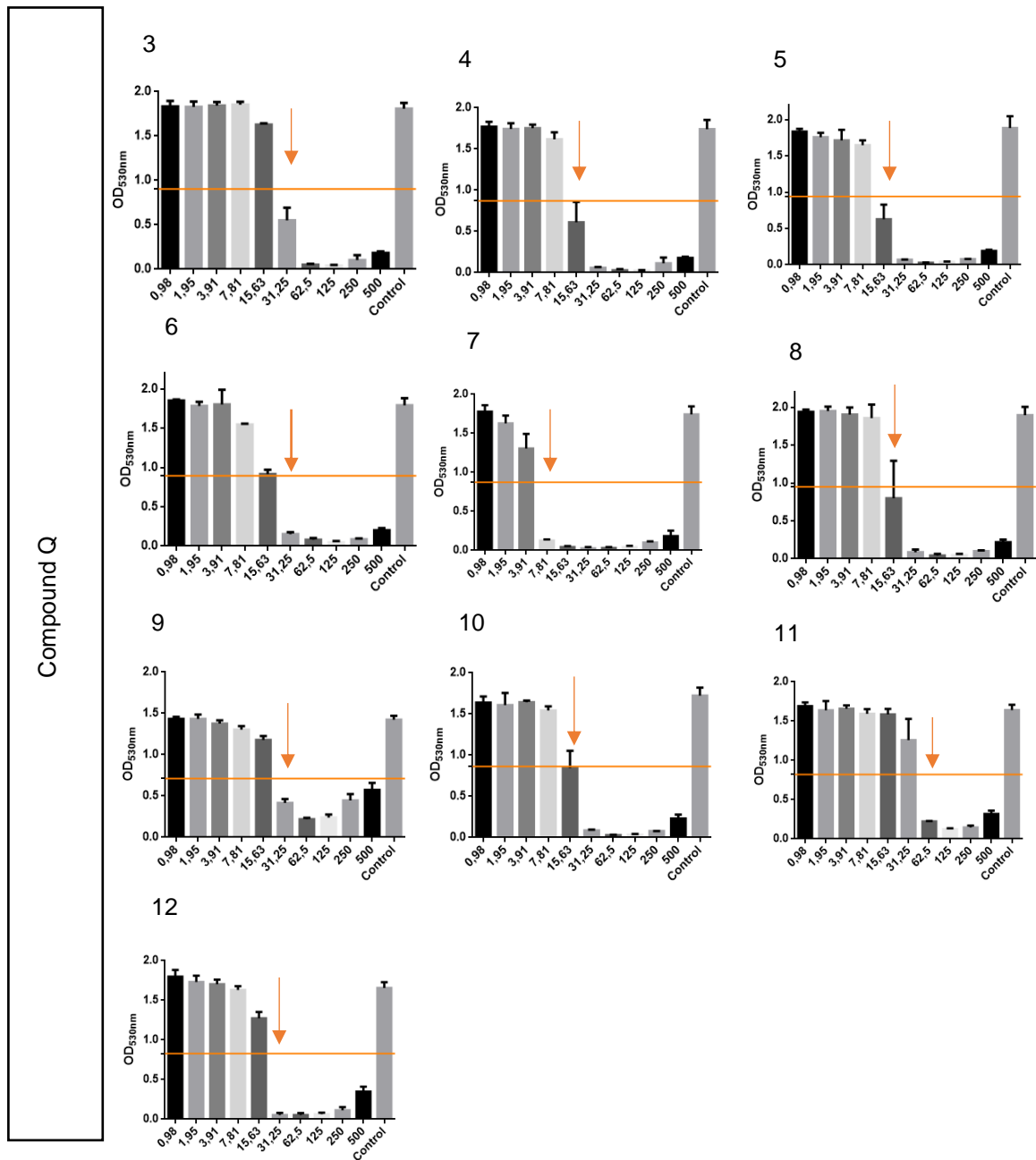


Figure 34 - Microdilution assay for all the complexes Q against the azole resistant isolates of *C. glabrata* (3-12). The MIC value is indicated by an orange arrow and the 50% reduction of the growth registered in the absence of the chemicals is indicated by the orange line

Annex F

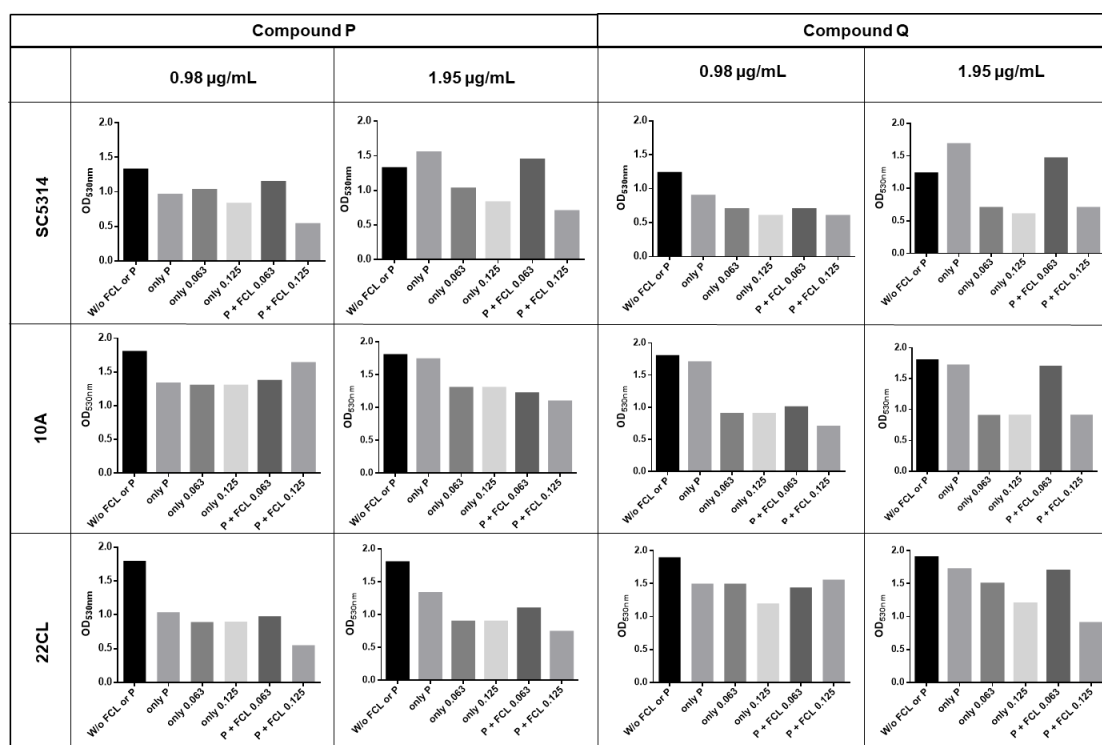


Figure 35 - Graphic representation of the ODs obtained in the assays to assess the effects of the potential synergistic combination of compound P or Q and fluconazole against *C. albicans* SC5314, 10A and 22CL strains. In the graphic are represented a control column (w/o FLC or A) with the growth medium without stress, the medium supplemented only with compounds P or Q, only with FLC and the conditions under which stresses were combined. Two non-inhibitory concentrations of compounds P and Q were used, 0.98 µg/mL, 1.95 µg/mL and two non-inhibitory concentrations of FLC were used, 0.063 µg/mL and 0.125 µg/mL.

Annex G

Table vi - Summary of the strategy followed in the functionalization of PCL coating.

PCL (w/v)	Solvent	DMSO	Compound and concentration (µg/mL)	Coating	Biological assay
8%	TFA	-	-	Broken coating	-
Conclusion: TFA releases toxic gases and causes burns.					
8%	Chloroform	-	-	Broken coating	-
Conclusion: high PCL concentration.					
4%	Chloroform	-	-	Intact coating	-
Conclusion: try different solvent to have another possibility in compound testing.					
4%	Dichloromethan	-	-	Intact coating	-
Conclusion: both solvents resulted, coatings were tested with compounds.					
4%	Chloroform	✓	P10, P100, Q10 and Q100	Functional coatings	✓
	Dichloromethan		P10 and Q10		

Annex H

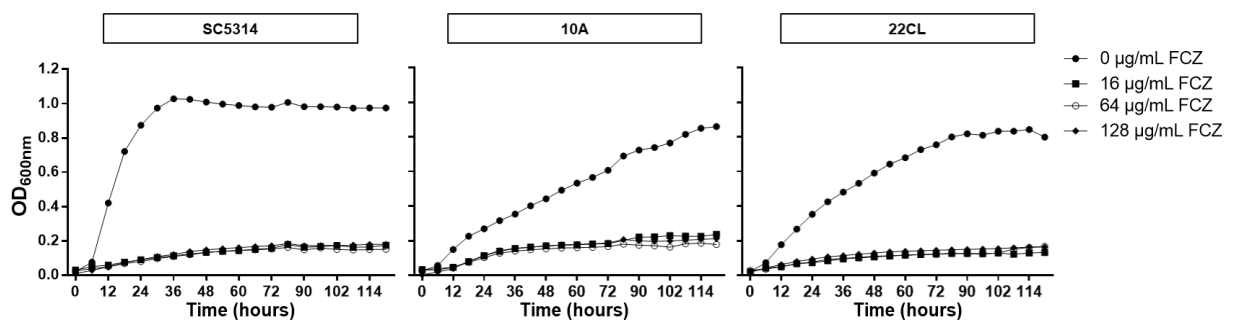


Figure 36 - Growth curve of SC5314, 10A and 22CL strains in RPMI growth medium (at pH 7). Growth of the different strains was based on the increase of OD_{600nm} of the culture. The growth curves shown are representative of at least three independent experiments that resulted in a similar growth pattern.